Height representation of XOR-Ising loops via bipartite dimers

Cédric Boutillier[*]   Béatrice de Tilière[*]

Abstract

The XOR-Ising model on a graph consists of random spin configurations on vertices of the graph obtained by taking the product at each vertex of the spins of two independent Ising models. In this paper, we explicitly relate loop configurations of the XOR-Ising model and those of a dimer model living on a decorated, bipartite version of the Ising graph. This result is proved for graphs embedded in compact surfaces of genus g. Using this fact, we then prove that XOR-Ising loops have the same law as level lines of the height function of this bipartite dimer model. At criticality, the height function is known to converge weakly in distribution to $\frac{1}{\sqrt{\pi}}$ a Gaussian free field [dT07b]. As a consequence, results of this paper shed a light on the occurrence of the Gaussian free field in the XOR-Ising model. In particular, they prove a discrete analogue of Wilson's conjecture [Wil11], stating that the scaling limit of XOR-Ising loops are "contour lines" of the Gaussian free field.

1 Introduction

The *double Ising model* consists of two Ising models, living on the same graph. It is related [KW71, Wu71, Fan72, Weg72] to other models of statistical mechanics, as the 8-vertex model [Sut70, FW70] and the Ashkin–Teller model [AT43]. In general, the two models may be interacting. However, in this paper, we consider the case of two non-interacting Ising models, defined on the dual $G^* = (V^*, E^*)$ of a graph $G = (V, E)$, having the same coupling constants $(J_{e^*})_{e^* \in E^*}$, where the graph G is embedded either in a compact, orientable, boundaryless surface Σ of genus $g \geq 0$, or in the plane.

We are interested in the polarization of the model [KB79], also referred to as the XOR-*Ising model* [Wil11] by Wilson. It is defined as follows: given a pair of spin configurations $(\sigma, \sigma') \in \{-1, 1\}^{V^*} \times \{-1, 1\}^{V^*}$, the XOR-*spin configuration* belongs to $\{-1, 1\}^{V^*}$

[*]Laboratoire de Probabilités et Modèles Aléatoires, UMR 7599, Université Pierre et Marie Curie, 4 place Jussieu, F-75005 Paris. E-mail: cedric.boutillier@upmc.fr, E-mail: beatrice.de_tiliere@upmc.fr

and is obtained by taking, at every vertex, the product of the spins. The interface between ± 1 spin configurations of the XOR-configuration is a loop configuration of the graph G. Using extensive simulations, Wilson [Wil11] finds that, when G is a specific simply connected domain of the plane, and when both Ising models are critical, XOR loop configurations seem to have the same limiting behavior as "contour lines" of the Gaussian free field, with heights of the contours spaced $\sqrt{2}$ times as far apart as they should be for the double dimer model on the square lattice. Similar conjectures involving SLE rather than the Gaussian free field, are obtained through conformal field theory [IR11, PS11]. Results of this paper explain the occurrence of the Gaussian free field in the XOR-Ising model and prove a discrete analogue of Wilson's conjecture.

The first part of this paper concentrates on finite graphs embedded in surfaces. We explicitly relate XOR loop configurations to loop configurations in a bipartite dimer model, implying in particular that both loop configurations have the same probability distribution. In the second part, we prove that this correspondence still holds for a large class of infinite planar graphs, the so-called *isoradial graphs* [Ken02, KS05], at criticality, and make the connection with Wilson's conjecture. Here is an outline.

Outline

Section 2. One of the tools required is a version of Kramers and Wannier's low/high-temperature duality [KW41a, KW41b] in the case of graphs embedded in surfaces of genus g, *with boundary*. In the literature, we did find versions of this duality for graphs embedded in surfaces of genus g [LG94], but we could not find versions taking into account boundaries. This is the subject of Propositions 2.1 and 2.2, it involves relative homology theory and the Poincaré–Lefschetz duality.

Sections 3 and 4 consist of the extension to general graphs embedded in a surface of genus g of an expansion due to Nienhuis [Nie84], which can be summarized as follows. Consider the low-temperature expansion of the double Ising model, *i.e.*, consider pairs of polygon configurations separating clusters of ± 1 spins of each spin configuration. Drawing both polygon configurations on G yields an edge configuration consisting of *monochromatic edges*, that is edges covered by exactly one of the two polygon configurations, and *bichromatic edges*, that is edges covered by both polygon configurations. Monochromatic edge configurations exactly correspond to XOR loop configurations, and separate the surface Σ into connected components $\Sigma_1, \ldots, \Sigma_N$. Inside each connected component, the law of bichromatic edge configurations is that of the low-temperature expansion of an Ising model with coupling constants that are doubled. As a consequence, the partition function of the double Ising model can be rewritten using XOR loop configurations and bichromatic edge configurations, see Proposition 3.3.

Fixing a monochromatic edge configuration, and applying low/high-temperature duality to the single Ising model corresponding to bichromatic edges, yields a rewriting of the double Ising partition function, as a sum over pairs of non-intersecting polygon configurations of the primal and dual graph, where primal polygon configurations exactly correspond to XOR loop configurations, see Proposition 4.2 and Corollary 4.3. Note that there are quite a few difficulties in the proofs, due to the fact that we work on a surface of genus g.

Proposition 1.1.
The double Ising partition function for a graph embedded on a surface of genus g can be rewritten as:

$$Z_{\text{d-Ising}}(G^*, J) = \mathcal{C}_{\text{I}} \sum_{\substack{\{(P, P^*) \in \mathcal{P}^0(G) \times \mathcal{P}^0(G^*): \\ P \cap P^* = \emptyset\}}} \left(\prod_{e \in P} \frac{2e^{-2J_{e^*}}}{1 + e^{-4J_{e^*}}} \right) \left(\prod_{e^* \in P^*} \frac{1 - e^{-4J_{e^*}}}{1 + e^{-4J_{e^*}}} \right),$$

where primal polygon configurations of $\mathcal{P}^0(G)$ are the XOR loop configurations, and $\mathcal{C}_{\mathrm{I}} = 2^{|V^*|+2g+1} \left(\prod_{e \in E} \cosh(2J_{e^*}) \right)$.

Section 5. In Section 5.1, we define the 6-vertex model on the medial graph G^{M} constructed from G. Reformulating an argument of Nienhuis [Nie84], we prove that the 6-vertex partition function can be written as a sum over non-intersecting pairs of polygon configurations of the primal and dual graphs.

In Section 5.2, we define the dimer model on the decorated, bipartite graph G^{Q} constructed from G. Then, we present the mapping between dimer configurations of G^{Q} and *free-fermionic* 6-vertex configurations of G^{M} [WL75, Dub11b]. Using both mappings, one assigns to every dimer configuration M a pair $\mathrm{Poly}(M) = (\mathrm{Poly}_1(M), \mathrm{Poly}_2(M))$ of non-intersecting primal and dual polygon configurations. The weights of the 6-vertex model chosen to match those of edges in the mixed contour expansion of the double Ising model satisfy the *free-fermionic* condition. As a consequence, we then obtain, see also Proposition 5.4:

Proposition 1.2. *The dimer model partition function $Z^0_{\mathrm{dimer}}(G^{\mathrm{Q}}, J)$ can be rewritten as:*

$$
Z^0_{\mathrm{dimer}}(G^{\mathrm{Q}}, J) = 2 \sum_{\substack{\{(P,P^*) \in \mathcal{P}^0(G) \times \mathcal{P}^0(G^*): \\ P \cap P^* = \emptyset\}}} \left(\prod_{e \in P} \frac{2e^{-2J_{e^*}}}{1 + e^{-4J_{e^*}}} \right) \left(\prod_{e^* \in P^*} \frac{1 - e^{-4J_{e^*}}}{1 + e^{-4J_{e^*}}} \right),
$$

where primal and dual polygon configurations of $\mathcal{P}^0(G) \times \mathcal{P}^0(G^*)$ are the Poly configurations.

Combining Proposition 1.1 and Proposition 1.2 yields the following, see also Theorem 5.5:

Theorem 1.3. *XOR loop configurations of the double Ising model on G^* have the same law as Poly_1 configurations of the corresponding dimer model on the bipartite graph G^{Q}:*

$$
\forall P \in \mathcal{P}^0(G), \quad \mathbb{P}_{\mathrm{d\text{-}Ising}}[\mathrm{XOR} = P] = \mathbb{P}^0_{\mathrm{Q}}[\mathrm{Poly}_1 = P].
$$

Remark 1.4. *In the paper [Dub11b], Dubédat relates a version of the double Ising model and the same bipartite dimer model in two ways. The first approach uses explicit mappings, most of which are present in the physics literature, and goes as follows. Consider a slightly different version of the double Ising model, with one model living on the primal graph G and the second on the dual graph G^*. This double Ising model can be mapped to an 8-vertex model [KW71, Wu71] on the medial graph. Using Fan and Wu's abelian duality, this 8-vertex model [FW70] can be mapped to a second 8-vertex on the same graph. When coupling constants of the two Ising models satisfy Kramers and Wannier's duality, the second 8-vertex model is in fact a free-fermionic 6-vertex model. The free-fermionic 6-vertex model can in turn be mapped to a bipartite dimer model, a result due to [WL75] in the case of the square lattice, and extended by [Dub11b] in the general lattice case. It can also be seen as a specific case of the mapping of the free-fermionic 8-vertex model to a non-bipartite dimer model of [FW70]. Note that this bipartite dimer model is the model of* quadri-tilings *studied by the second author in [dT07a] and [dT07b].*

When performing the different steps of the mapping, Dubédat keeps track of order/disorder variables, in the vein of [KC71]. Using results of a previous paper of his [Dub11a], this allows him to compute critical correlators in the plane. For simply connected regions, this result has independently been obtained by Chelkak, Hongler and Izyurov [CHI12].

Our goal here is different, since we aim at keeping track of XOR-configurations. This information is not directly available in the above approach. Indeed Fan and Wu's abelian duality for the 8-vertex model can be compared to a high-temperature expansion, where configurations cannot be interpreted using the initial model. Note that expanding and recombining the identities of [Dub11b] involving correlators, one can recover the identity in law of Theorem 1.3; this proves the existence of a coupling between the two models, which we explicitly provide in this paper.

The second approach uses transformations on matrices. The partition function of the double Ising model can be expressed using the determinant of the Kasteleyn matrix of the Fisher graph [Fis66]; whereas the partition function of the bipartite dimer model can be expressed using the Kasteleyn matrix of the graph G^Q. Dubédat shows that the two matrices are related through transformations not affecting the determinant. Using the fact that the partition function of the double Ising model is also related to the determinant of the Kac–Ward matrix [KW52], Cimasoni and Duminil-Copin use the same approach to relate the Kac–Ward matrix to the matrix of the same bipartite dimer model [CDC13]. Their purpose is to identify the critical point of general bi-periodic Ising models, see also Li [Li10, Li12] for the case of the square lattice with arbitrary fundamental domain.

However, the above transformations on matrices are not easily interpreted in terms of transformations on configurations, and the relation to XOR-configurations is not straightforward.

Using Nienhuis' mapping [Nie84], the main contribution of this paper is to provide a coupling between the double Ising model and the bipartite dimer model, which keeps track of XOR loop configurations, and is valid for graphs embedded in surfaces of genus g.

Section 6. Suppose now that the two Ising models are critical and defined on the dual of an infinite isoradial graph G filling the whole plane, see Section 6.1 for definitions. Then, the dimer model on the corresponding graph G^Q is also critical in the dimer sense. Using the locality property of both probability measures on Ising [BdT11], and dimer configurations [dT07b] on isoradial graphs at criticality, we prove that the equality in law stated in Theorem 1.3 still holds in this infinite context. See Theorem 6.2.

Section 7. The graph G^Q being bipartite, using a height function denoted h, dimer configurations can naturally be interpreted as discrete random interfaces. Our second theorem, see also Theorem 7.5, proves the following

Theorem 1.5. *XOR loop configurations of the double Ising model defined on G^* have the same law as level lines of the restriction of the height function h to vertices of the dual graph G^*.*

Theorem 1.5 can be interpreted as a proof of Wilson's conjecture mentioned above (see Section 7.2 for a precise statement) in the discrete setting, since it is known that the height function h, seen as a random distribution, converges in law in the scaling limit to $\frac{1}{\sqrt{\pi}}$ times the Gaussian free field in the plane [dT07b]. In particular, we explain the special value of the spacing. It would yield a complete proof of the conjecture if we could overcome the same technical obstacles as those of the proof of the convergence of double dimer loops to CLE_4.

2 Ising model on graphs embedded in surfaces

In this section, we let G be a graph embedded in a compact, orientable, boundaryless surface of genus g ($g \geq 0$), and G^* be its dual graph. The embedding of G^* is chosen such that dual vertices are in the interior of the corresponding faces.

Fix some integer $p \geq 0$, and suppose first that $p \geq 1$. For every $i \in \{0, \dots, p-1\}$, let B_i be a union of closed faces of G homeomorphic to a disc, such that $\forall i \neq j$, $B_i \cap B_j = \emptyset$. Denote by Σ the surface of genus g from which the union of the interiors of B_i's is removed. Then Σ is a compact, orientable surface of genus g, with boundary $\partial\Sigma = \partial B_0 \cup \cdots \partial B_{p-1}$. When $p = 0$, then Σ is the compact, orientable, boundaryless surface of genus g in which the graph G is embedded.

Let $G_\Sigma = (V_\Sigma, E_\Sigma)$ be the subgraph of G defined as follows: V_Σ consists of vertices of $V \cap \Sigma$; and E_Σ consists of edges of E joining vertices of V_Σ, from which edges on the boundary $\partial\Sigma$ are removed. Let $G_\Sigma^* = (V_\Sigma^*, E_\Sigma^*)$ be the subgraph of G^* whose vertices are vertices of $V^* \cap \Sigma$, and whose edges are edges of G^* joining vertices of V_Σ^*; see Figure 1 for an example. Note that the graph G_Σ^* contains all edges dual to edges of G_Σ, i.e., there is a bijection between primal edges of G_Σ and dual edges of G_Σ^*. Note that when $p = 0$, $G_\Sigma = G$ and $G_\Sigma^* = G^*$.
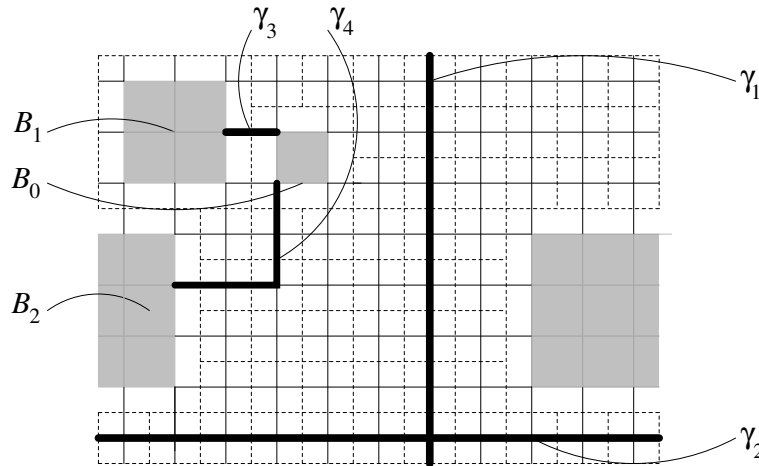

Figure 1: The graph G is a piece of $\mathbb{Z}^2$ embedded in the torus. The union of faces $(B_i)_{i \in \{0,1,2\}}$ is pictured in light grey. The graph G_Σ consists of black plain lines, and the dual graph G_Σ^* of black dotted lines. The paths $(\gamma_i)_{i=1}^4$ defining *defects* of Section 2.1 are drawn in thick black lines.

Fix a collection of positive constants $(J_{e^*})_{e^* \in E^*}$ attached to edges of G^*, referred to as *coupling constants*. The *Ising model on G_Σ^* with free boundary conditions and coupling constants* (J_{e^*}) is defined as follows. A *spin configuration* σ of G_Σ^* is a function of the vertices of V_Σ^* with values in $\{-1, +1\}$. The probability of occurrence of a spin configuration σ is given by the *Ising Boltzmann measure*, denoted $\mathbb{P}_{\text{Ising}}$, and defined by:

$$\forall \sigma \in \{-1, 1\}^{V_\Sigma^*}, \quad \mathbb{P}_{\text{Ising}}(\sigma) = \frac{1}{Z_{\text{Ising}}(G_\Sigma^*, J)} \exp\left(\sum_{e^* = u^* v^* \in E_\Sigma^*} J_{e^*} \sigma_{u^*} \sigma_{v^*}\right),$$

where $Z_{\text{Ising}}(G_\Sigma^*, J) = \sum_{\sigma \in \{-1,+1\}^{V_\Sigma^*}} \exp\left(\sum_{e^* = u^* v^* \in E_\Sigma^*} J_{e^*} \sigma_{u^*} \sigma_{v^*}\right)$ is the *Ising partition func-*

tion. Note that to simplify notation, the inverse temperature is included in the coupling constants.

2.1 Ising model with defect lines

When $p \geq 1$, let $N = 2g + p - 1$, and when $p = 0$, let $N = 2g$. We now define 2^N versions of the original Ising model. Let $\underline{\gamma}_1, \cdots, \underline{\gamma}_N$ be N unoriented paths consisting of edges of the primal graph G_Σ; see Figure 1 for an example, where

- for every $i \in \{1, \ldots, g\}$, the paths $\underline{\gamma}_{2i-1}, \underline{\gamma}_{2i}$ wind around the i-th handle in two transverse directions,
- when $p \geq 2$, for every $i \in \{1, \ldots, p-1\}$, the path $\underline{\gamma}_{2g+i}$ joins ∂B_0 and ∂B_i.

The paths γ_i's are thought as sets of edges. Let $\underline{\epsilon}$ be one of the 2^N possible "unions" of paths $\widehat{\cup}_{i \in I} \underline{\gamma}_i$, where $I \subset \{1, \ldots, N\}$ and $\widehat{\cup}$ means that an edge with multiplicity k is present iff $k \equiv 1 \mod 2$. Then, we change the sign of coupling constants of dual edges intersecting with $\underline{\epsilon}$. Spin configurations are defined as above, and so is the probability measure on spin configurations. This defines the *Ising model with coupling constants* (J_{e^*}) *and defect condition* $\underline{\epsilon}$.

In fact, the appropriate framework for defining the Ising model with defects, is relative homology theory, see Appendices A.2, A.3, and A.4. The *first homology group of* Σ *relative to its boundary* $\partial\Sigma$ is denoted by $H_1(\Sigma, \partial\Sigma; \mathbb{Z}/2\mathbb{Z})$. The collection of paths $(\underline{\gamma}_1, \ldots, \underline{\gamma}_N)$ defined above, is a representative of a basis $\Gamma = (\gamma_1, \ldots, \gamma_N)$ of the first relative homology group $H_1(\Sigma, \partial\Sigma; \mathbb{Z}/2\mathbb{Z})$ seen as a $\mathbb{Z}/2\mathbb{Z}$-vector space. In the case where $p = 0$, $\partial\Sigma = \emptyset$ and the first homology group of Σ relative to its boundary is simply the first homology group.

Let ϵ denote the relative homology class of $\underline{\epsilon}$ in $H_1(\Sigma, \partial\Sigma; \mathbb{Z}/2\mathbb{Z})$. Then, it will be clear from the low-temperature expansion of Section 2.2 that the partition function is independent of the choice of basis and of the choice of representative of ϵ. As a consequence, we refer to this model as the *Ising model with coupling constants* (J_{e^*}) *and defect condition* ϵ, and denote by $Z^{\epsilon}_{\text{Ising}}(G^*_\Sigma, J)$ the corresponding partition function. Nevertheless, since we want the change of signs of coupling constants to be well defined throughout the paper, we fix representatives of relative homology classes in $H_1(\Sigma, \partial\Sigma; \mathbb{Z}/2\mathbb{Z})$, using the collection of paths $\underline{\gamma}_1, \ldots, \underline{\gamma}_N$ defined above. Note that the original Ising model introduced has defect condition $\epsilon = 0$ and $\underline{\epsilon}$ is empty. Note also that this treatment is completely equivalent to considering the connected components of the boundary as the boundary of marked faces, and allowing insertion of disorder operators on these marked faces. However, the formulation in terms of defect conditions is natural in our context: the graphs on which the Ising model with defect conditions live, arise from the surgery of a larger graph embedded in a surface, and as such, their boundary have a real geometric meaning.

2.2 Low- and high-temperature expansion

Proposition 2.1 below extends the *low-temperature expansion* of Kramers and Wannier [KW41a, KW41b] to the case of graphs embedded on a compact, orientable surface with boundary. It consists of rewriting the Ising partition function as a sum over polygon configurations of the graph G_Σ, "separating" clusters of ± 1 spins; see Figure 2 (left) for an example.

A *polygon configuration* of G_Σ is a subset of edges of G_Σ, such that vertices not on the boundary $\partial\Sigma$ are incident to an even number of edges. There is no restriction for vertices on the boundary $\partial\Sigma$. Let us denote by $\mathcal{P}(G_\Sigma)$ the set of polygon configurations of G_Σ.
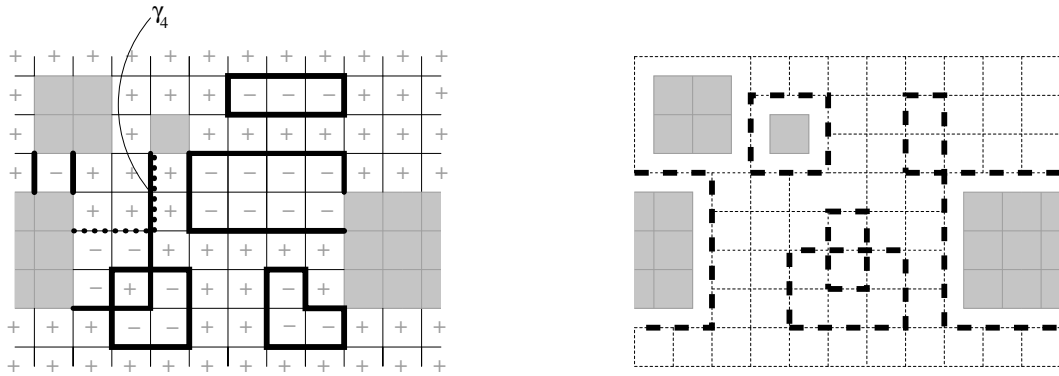
Figure 2: Left: polygon configuration of G_Σ corresponding to a spin configuration of the Ising model with defect condition $\underline{\epsilon} = \gamma_4$. Right: polygon configuration of G_Σ^*.

Let ϵ be an element of $H_1(\Sigma, \partial\Sigma; \mathbb{Z}/2\mathbb{Z})$, and let $\mathcal{P}^\epsilon(G_\Sigma)$ denote the set of polygon configurations of G_Σ whose relative homology class in $H_1(\Sigma, \partial\Sigma; \mathbb{Z}/2\mathbb{Z})$ is ϵ, meaning in particular that, for every i, the number of edges on ∂B_i has the same parity as ϵ_{2g+i}.

This defines a partition of $\mathcal{P}(G_\Sigma)$:

$$\mathcal{P}(G_\Sigma) = \bigcup_{\epsilon \in H_1(\Sigma, \partial\Sigma; \mathbb{Z}/2\mathbb{Z})} \mathcal{P}^\epsilon(G_\Sigma).$$

Proposition 2.1 (Low-temperature expansion).
For every relative homology class $\epsilon \in H_1(\Sigma, \partial\Sigma; \mathbb{Z}/2\mathbb{Z})$,

$$Z_{\mathrm{Ising}}^\epsilon(G_\Sigma^*, J) = 2 \Big(\prod_{e \in E_\Sigma} e^{J_{e^*}} \Big) \sum_{P \in \mathcal{P}^\epsilon(G_\Sigma)} \prod_{e \in P} e^{-2J_e^*}. \tag{2.1}$$

Proof. Suppose for the moment that ϵ is the class $0 \in H_1(\Sigma, \partial\Sigma; \mathbb{Z}/2\mathbb{Z})$, so that we deal with the usual Ising model. Using the identity (2.2) below, one can rewrite the partition function as a statistical sum over polygon configurations separating clusters of ± 1 spins: if σ_{u^*} and σ_{v^*} are two neighboring spins of an edge $e^* = u^*v^*$, then

$$e^{J_{e^*}\sigma_{u^*}\sigma_{v^*}} = e^{J_{e^*}} \left(\delta_{\{\sigma_{u^*}=\sigma_{v^*}\}} + e^{-2J_{e^*}} \delta_{\{\sigma_{u^*}\neq\sigma_{v^*}\}} \right). \tag{2.2}$$

When injecting the right hand side in the expression of the Ising partition function, the product over dual edges e^* of $e^{J_{e^*}}$ can be factored out. Since primal and dual edges are in bijection, this can also be written as a product over primal edges. Then, expanding the product, we get a product of contributions for all edges separating two neighboring spins with opposite signs. These edges form a polygon configuration P^0 of G_Σ separating clusters of ± 1 spins. As a consequence P^0 has homology class 0, *i.e.*, P^0 belongs to $\mathcal{P}^0(G_\Sigma)$.

Conversely, any polygon configuration of $\mathcal{P}^0(G_\Sigma)$ is the boundary of exactly two spin configurations, one obtained from the other by negating all spins, which explains the factor 2 on the right hand side of (2.1).

Suppose now that $\epsilon \neq 0$. In the Ising model with defect condition ϵ, coupling constants of edges crossing paths of the representative $\underline{\epsilon}$ are negated. For these edges, the relation (2.2) should be replaced by the following:

$$e^{-J_{e^*}\sigma_{u^*}\sigma_{v^*}} = e^{J_{e^*}} \left(\delta_{\{\sigma_{u^*}\neq\sigma_{v^*}\}} + e^{-2J_{e^*}} \delta_{\{\sigma_{u^*}=\sigma_{v^*}\}} \right).$$

Note that, when comparing to (2.2), the two Kronecker symbols have been exchanged. As a consequence, the construction of polygon configurations as above is slightly modified: the edge configuration, denoted by P, constructed from a spin configuration is obtained from P^0 by switching the state of every edge e in $\underline{\epsilon}$; see Figure 2 (left). Then, the relative homology class of P in $H_1(\Sigma, \partial\Sigma; \mathbb{Z}/2\mathbb{Z})$ is:

$$[P] = [P^0] + [\underline{\epsilon}] = 0 + \epsilon = \epsilon.$$

As a consequence P belongs to $\mathcal{P}^\epsilon(G_\Sigma)$ and this, independently of the choice of representative of ϵ. Conversely, any element of $\mathcal{P}^\epsilon(G_\Sigma)$ is obtained twice in this way. □

For the sequel, it is useful to introduce a symbol for the sum over polygon configurations of the low-temperature expansion. For $\epsilon \in H_1(\Sigma, \partial\Sigma; \mathbb{Z}/2\mathbb{Z})$, define

$$Z_{\mathrm{LT}}^\epsilon(G_\Sigma, J) = \sum_{P \in \mathcal{P}^\epsilon(G_\Sigma)} \Big(\prod_{e \in P} e^{-2J_{e^*}} \Big).$$

The partition function of the Ising model with defect condition ϵ can thus be rewritten as:

$$Z_{\mathrm{Ising}}^\epsilon(G_\Sigma^*, J) = 2 \Big(\prod_{e \in E_\Sigma} e^{J_{e^*}} \Big) Z_{\mathrm{LT}}^\epsilon(G_\Sigma, J).$$

Proposition 2.2 below extends the *high-temperature expansion* [KW41a, KW41b, Wan45] to the case of graphs embedded in a compact, orientable surface with boundary. It consists of rewriting the Ising partition function as a sum over polygon configurations of the graph G_Σ^*, this time. In this case, polygon configurations do not have a simple interpretation in terms of spin configurations.

A *polygon configuration* of G_Σ^* (or simply *dual polygon configuration*) is a subset of edges such that each vertex of G_Σ^* is incident to an even number of edges, see Figure 2 (right) for an example. It is thus a union of closed cycles on G_Σ^*. Let us denote by $\mathcal{P}(G_\Sigma^*)$ the set of polygon configurations of G_Σ^*.

Let $H_1(\Sigma; \mathbb{Z}/2\mathbb{Z})$ be the first homology group of Σ, see Appendices A.1, A.3 and A.4. Then, to each dual polygon configuration is assigned its homology class in $H_1(\Sigma; \mathbb{Z}/2\mathbb{Z})$. For every $\tau \in H_1(\Sigma; \mathbb{Z}/2\mathbb{Z})$, we let $\mathcal{P}^\tau(G_\Sigma^*)$ denote the set of dual polygon configurations restricted to having homology class τ in $H_1(\Sigma; \mathbb{Z}/2\mathbb{Z})$. This defines a partition of $\mathcal{P}(G_\Sigma^*)$:

$$\mathcal{P}(G_\Sigma^*) = \bigcup_{\tau \in H_1(\Sigma; \mathbb{Z}/2\mathbb{Z})} \mathcal{P}^\tau(G_\Sigma^*).$$

Proposition 2.2 (High-temperature expansion).
For every relative homology class $\epsilon \in H_1(\Sigma, \partial\Sigma; \mathbb{Z}/2\mathbb{Z})$,

$$Z_{\mathrm{Ising}}^\epsilon(G_\Sigma^*, J) = 2^{|V_\Sigma^*|} \Big(\prod_{e \in E_\Sigma} \cosh(J_{e^*}) \Big) \cdot \sum_{\tau \in H_1(\Sigma; \mathbb{Z}/2\mathbb{Z})} \Big[(-1)^{(\tau|\epsilon)} \sum_{P^* \in \mathcal{P}^\tau(G_\Sigma^*)} \Big(\prod_{e^* \in P^*} \tanh(J_{e^*}) \Big) \Big],$$
(2.3)

where $(\tau|\epsilon)$ is the intersection form *evaluated at τ and ϵ: it is the parity of the number of intersections of any representative of τ and any representative of ϵ.*

For details on the intersection form, see Appendix A.5.

Proof. This result is based on yet another way of rewriting the quantity $e^{\pm J_{e^*} \sigma_{u^*} \sigma_{v^*}}$ for a dual edge $e^* = u^* v^*$ of E_Σ^*.

$$
\begin{aligned}
e^{\pm J_{e^*} \sigma_{u^*} \sigma_{v^*}} &= \cosh J_{e^*} \pm \sigma_{u^*} \sigma_{v^*} \sinh J_{e^*} \\
&= \cosh J_{e^*} \left(1 \pm \sigma_{u^*} \sigma_{v^*} \tanh J_{e^*} \right).
\end{aligned}
$$
(2.4)

The partition function is expanded into a sum of monomials in $(\sigma_{u^*})_{u^* \in V_\Sigma^*}$. In the expansion, the spin variables come by pairs of neighbors $\sigma_{u^*}\sigma_{v^*}$ and thus can be formally identified with the dual edge connecting u^* and v^*, associated with a weight $\pm \tanh J_{e^*}$. Each monomial is then interpreted as a subgraph of G_Σ^*, the degree of σ_{u^*} being the degree of u^* in the corresponding edge configuration. Because of the symmetry $\sigma \leftrightarrow -\sigma$, when re-summing over spin configurations σ, only terms having even degree in each variable remain, giving a factor 2 per dual vertex, and other contributions cancel. As a consequence, the contributing monomials correspond to even subgraphs $i.e.$, polygon configurations of $\mathcal{P}(G_\Sigma^*)$.

We now determine the sign of dual polygon configurations. Fix $\tau \in H_1(\Sigma; \mathbb{Z}/2\mathbb{Z})$ and a dual polygon configuration $P^* \in \mathcal{P}^\tau(G_\Sigma^*)$. Then, edges of P^* carrying a negative weight are exactly those crossing edges of $\underline{\epsilon}$. As a consequence, the sign of the contribution of P^* corresponds to (-1) to the parity of the number of edges of P^* intersecting with $\underline{\epsilon}$, this is exactly given by $(\tau|\epsilon)$. The dual polygon configuration P^* thus has sign $(-1)^{(\tau|\epsilon)}$. □

As in the case of the low-temperature expansion, it is useful to introduce a notation for the sum over dual polygon configurations of the high-temperature expansion. For $\tau \in H_1(\Sigma; \mathbb{Z}/2\mathbb{Z})$, define:

$$Z_{\mathrm{HT}}^\tau(G_\Sigma^*, J) = \sum_{P^* \in \mathcal{P}^\tau(G_\Sigma^*)} \Big(\prod_{e^* \in P^*} \tanh(J_{e^*}) \Big).$$

The relation between (2.1) and (2.3) can then be rewritten in the following compact form. For every relative homology class $\epsilon \in H_1(\Sigma, \partial\Sigma; \mathbb{Z}/2\mathbb{Z})$:

$$Z_{\mathrm{LT}}^\epsilon(G_\Sigma, J) = 2^{|V_\Sigma^*|-1} \left(\prod_{e \in E_\Sigma} \frac{\cosh(J_{e^*})}{e^{J_{e^*}}} \right) \sum_{\tau \in H_1(\Sigma; \mathbb{Z}/2\mathbb{Z})} \Big[(-1)^{(\tau|\epsilon)} Z_{\mathrm{HT}}^\tau(G_\Sigma^*, J) \Big]. \qquad (2.5)$$

Remark 2.3. *Relation* (2.5) *can be inverted using the orthogonality identity:*

$$\sum_{\epsilon \in H_1(\Sigma, \partial\Sigma; \mathbb{Z}/2\mathbb{Z})} (-1)^{(\tau|\epsilon)}(-1)^{(\tau'|\epsilon)} = 2^N \delta_{\tau,\tau'}, \qquad (2.6)$$

where $N = 2g + p - 1$ when $p \geq 1$, and $N = 2g$ when $p = 0$. This orthogonality relation is proved as follows. The summand can be rewritten as $(-1)^{(\tau-\tau'|\epsilon)}$. The application $\epsilon \mapsto (-1)^{(\tau-\tau'|\epsilon)}$ is a group homomorphism from $H_1(\Sigma, \partial\Sigma; \mathbb{Z}/2\mathbb{Z})$ to $\mathbb{Z}/2\mathbb{Z}$. When $\tau = \tau'$, this application is constant, equal to 1, all terms in the sum (2.6) *equal 1, and the total sum equals 2^N. Otherwise, since the intersection pairing is non-degenerate (see Appendix A.5), the application $\epsilon \mapsto (-1)^{(\tau-\tau'|\epsilon)}$ takes the values 1 and -1 the same number of times, and the sum* (2.6) *is zero. Using this identity, we obtain the inverted version of relation* (2.5)*:*

$$Z_{\mathrm{HT}}^\tau(G_\Sigma^*, J) = 2^{-N-|V_\Sigma^*|+1} \left(\prod_{e \in E_\Sigma} \frac{e^{J_{e^*}}}{\cosh(J_{e^*})} \right) \sum_{\epsilon \in H_1(\Sigma, \partial\Sigma; \mathbb{Z}/2\mathbb{Z})} \Big[(-1)^{(\tau|\epsilon)} Z_{\mathrm{LT}}^\epsilon(G_\Sigma, J) \Big].$$

3 Double Ising model on a boundaryless surface of genus g

In this section, we let G be a graph embedded in a compact, orientable, boundaryless surface Σ of genus g, and G^* denote its dual graph. Since Σ has no boundary, the first homology group $H_1(\Sigma, \partial\Sigma; \mathbb{Z}/2\mathbb{Z})$ of Σ relative to its boundary is identified with the first homology group $H_1(\Sigma, \mathbb{Z}/2\mathbb{Z})$.

Instead of one Ising model on G^*, we now consider two copies of the Ising model, say a red one and a blue one, with the same coupling constants (J_{e^*}). These two models

are not taken to be completely independent: we require that they have the same defect conditions, *i.e.*, we ask that polygon configurations coming from the low-temperature expansion of both spin configurations have the same homology class.

More precisely, from the point of view of the low-temperature expansion, we are interested in the probability measure $\mathbb{P}_{\text{d-Ising}}$, on $\mathfrak{P} := \bigcup_{\epsilon \in H_1(\Sigma; \mathbb{Z}/2\mathbb{Z})} \mathcal{P}^\epsilon(G) \times \mathcal{P}^\epsilon(G)$, defined by, for every $(P_{\text{red}}, P_{\text{blue}}) \in \mathfrak{P}$:

$$\mathbb{P}_{\text{d-Ising}}(P_{\text{red}}, P_{\text{blue}}) = \frac{\mathcal{C}\left(\prod_{e \in P_{\text{red}}} e^{-2J_{e^*}}\right)\left(\prod_{e \in P_{\text{blue}}} e^{-2J_{e^*}}\right)}{Z_{\text{d-Ising}}(G^*, J)},$$

where $\mathcal{C} = \left(2 \prod_{e \in E} e^{J_{e^*}}\right)^2$, and the partition function $Z_{\text{d-Ising}}(G^*, J)$ is given by:

$$\begin{aligned}
Z_{\text{d-Ising}}(G^*, J) &= \sum_{\epsilon \in H_1(\Sigma; \mathbb{Z}/2\mathbb{Z})} \sum_{(P_{\text{red}}, P_{\text{blue}}) \in \mathcal{P}^\epsilon(G) \times \mathcal{P}^\epsilon(G)} \mathcal{C}\left(\prod_{e \in P_{\text{red}}} e^{-2J_{e^*}}\right)\left(\prod_{e \in P_{\text{blue}}} e^{-2J_{e^*}}\right) \\
&= \sum_{\epsilon \in H_1(\Sigma; \mathbb{Z}/2\mathbb{Z})} (Z^\epsilon_{\text{Ising}}(J))^2.
\end{aligned}$$

Given a pair $(P_{\text{red}}, P_{\text{blue}}) \in \mathfrak{P}$, and looking at the superimposition $P_{\text{red}} \cup P_{\text{blue}}$ on G, one defines two new edge configurations:

- $\text{Mono}(P_{\text{red}}, P_{\text{blue}})$: consisting of monochromatic edges of the superimposition $P_{\text{red}} \cup P_{\text{blue}}$, *i.e.*, edges covered by exactly one of the polygon configuration;
- $\text{Bi}(P_{\text{red}}, P_{\text{blue}})$: consisting of bichromatic edges of the superimposition, *i.e.*, edges covered by both polygon configurations.

Edges which are not in the two configurations above are covered neither by P_{blue} nor by P_{red}. In Sections 3.1 and 3.2 below, we characterize these two sets of edges.

3.1 Monochromatic edges

Let $\epsilon \in H_1(\Sigma; \mathbb{Z}/2\mathbb{Z})$, and consider a pair of polygon configurations $(P_{\text{red}}, P_{\text{blue}})$ in $\mathcal{P}^\epsilon(G) \times \mathcal{P}^\epsilon(G)$. Then, it can be realized as four pairs of Ising spin configurations $(\pm\sigma, \pm\sigma')$, each with defect type ϵ, where coupling constants are negated along the representative $\underline{\epsilon}$ of ϵ, chosen in Section 2.1.

Following Wilson [Wil11], to each of the four pairs of spin configurations, one assigns an XOR-*spin configuration* defined as follows: at every vertex, the XOR-spin is the product of the Ising-spins at that same vertex.

Note that the four pairs of spin configurations yield two distinct XOR-spin configurations, one being obtained from the other by negating all spins. As a consequence, both XOR-spin configurations have the same polygon configuration separating clusters of ± 1 spins, meaning that this polygon configuration is independent of the choice of $(\pm\sigma, \pm\sigma')$ realizing $(P_{\text{red}}, P_{\text{blue}})$, let us denote it by $\text{XOR}(P_{\text{red}}, P_{\text{blue}})$. Note also, that although the definition of σ and σ' depends on the particular choice of representative $\underline{\epsilon}$, the XOR polygon configuration does not: it is defined intrinsically from $(P_{\text{red}}, P_{\text{blue}})$.

Lemma 3.1. *For every pair of polygon configurations $(P_{red}, P_{blue}) \in \mathfrak{P}$, the monochromatic edge configuration $\text{Mono}(P_{red}, P_{blue})$ is exactly the XOR loop configuration $\text{XOR}(P_{red}, P_{blue})$. In particular, it is a polygon configuration of $\mathcal{P}^0(G)$.*

Proof. Fix a pair of red and blue polygon configurations $(P_{\text{red}}, P_{\text{blue}}) \in P^\epsilon(G) \times P^\epsilon(G)$ for some $\epsilon \in H_1(\Sigma; \mathbb{Z}/2\mathbb{Z})$. Let (σ, σ') be one of the four pairs of spin configurations whose low-temperature expansion is $(P_{\text{red}}, P_{\text{blue}})$. We need to show that, for every edge e of G,

e is monochromatic, if and only if XOR-spins at vertices u^*, v^* of the dual edge e^* are distinct. Suppose that e does not belong to $\underline{\epsilon}$. Then,

- the edge e is red only $\Leftrightarrow$ $\sigma_{u^*} \neq \sigma_{v^*}$ and $\sigma'_{u^*} = \sigma'_{v^*}$,
- the edge e is blue only $\Leftrightarrow$ $\sigma_{u^*} = \sigma_{v^*}$ and $\sigma'_{u^*} \neq \sigma'_{v^*}$.

If e belongs to $\underline{\epsilon}$, the two above conditions hold with colors exchanged. In all cases, e is monochromatic if and only if XOR spins at vertices u^* and v^* are distinct.

Being the boundary of some domain, the set of monochromatic edges must be a polygon configuration of G, with homology class 0. $\qquad\square$

3.2 Bichromatic edge configurations

Before describing features of bichromatic edge configurations, we recall some general facts. A polygon configuration P of the graph G separates the surface Σ into n_P connected components $\Sigma_1, \ldots, \Sigma_{n_P}$, where $n_P \geq 1$. For every $i \in \{1, \ldots, n_P\}$, Σ_i is a surface of genus g_i with boundary $\partial\Sigma_i$. The boundary is either empty or consists of cycles of Σ.

As in Section 2, G_{Σ_i} denotes the subgraph of G, whose vertex set V_{Σ_i} is $V \cap \Sigma_i$, and whose edge set E_{Σ_i} consists of edges of E joining vertices of V_{Σ_i}, from which edges on the boundary $\partial\Sigma_i$ are removed. The dual graph is denoted by $G^*_{\Sigma_i}$.

Recall that $H_1(\Sigma_i, \partial\Sigma_i; \mathbb{Z}/2\mathbb{Z})$ denotes the first homology group of Σ_i relative to its boundary. Consider the morphism $\Pi_i = \Pi_{\Sigma, \Sigma_i}$, from $H_1(\Sigma; \mathbb{Z}/2\mathbb{Z})$ to $H_1(\Sigma_i, \partial\Sigma_i; \mathbb{Z}/2\mathbb{Z})$ defined as follows: for every $\epsilon \in H_1(\Sigma; \mathbb{Z}/2\mathbb{Z})$, $\Pi_i(\epsilon)$ is the homology class in $H_1(\Sigma_i, \partial\Sigma_i; \mathbb{Z}/2\mathbb{Z})$ of the restriction of any representative $\underline{\epsilon}$ of ϵ to Σ_i, see Appendix A.6 for details.

The following lemma characterizes bichromatic edge configurations.

Lemma 3.2. *Fix* $\epsilon \in H_1(\Sigma; \mathbb{Z}/2\mathbb{Z})$, *and let* $P \in \mathcal{P}^0(G)$ *be a polygon configuration, separating the surface* Σ *into connected components* $\Sigma_1, \ldots, \Sigma_{n_P}$.

- *If there exists a pair of polygon configurations* $(P_{red}, P_{blue}) \in \mathcal{P}^\epsilon(G) \times \mathcal{P}^\epsilon(G)$ *such that* $\mathrm{Mono}(P_{red}, P_{blue}) = P$; *then, for every* $i \in \{1, \ldots, n_P\}$, *the restriction of bichromatic edges to* G_{Σ_i} *is the low-temperature expansion of an Ising configuration on* $G^*_{\Sigma_i}$, *with coupling constants* $(2J_{e^*})$ *and defect condition* $\Pi_i(\epsilon)$. *As a consequence, it is a polygon configuration in* $\mathcal{P}^{\Pi_i(\epsilon)}(G_{\Sigma_i})$.
- *Given, for every* $i \in \{1, \ldots, n_P\}$, *a polygon configuration* $P_i \in \mathcal{P}^{\Pi_i(\epsilon)}(G_{\Sigma_i})$, *there are* $2^{n_P - 1}$ *pairs* $(P_{red}, P_{blue}) \in \mathcal{P}^\epsilon(G) \times \mathcal{P}^\epsilon(G)$ *such that* $\mathrm{Mono}(P_{red}, P_{blue}) = P$ *and such that, for every* $i \in \{1, \ldots, n_P\}$, *the restriction of bichromatic edges to* G_{Σ_i} *is* P_i.

Proof.

- Suppose that there exists a pair of polygon configurations $(P_{\text{red}}, P_{\text{blue}})$ of $\mathcal{P}^\epsilon(G) \times \mathcal{P}^\epsilon(G)$ such that $\mathrm{Mono}(P_{\text{red}}, P_{\text{blue}}) = P$. Then, for every $i \in \{1, \ldots, n_P\}$, the restriction of bichromatic edges to G_{Σ_i} exactly consists of the restriction to G_{Σ_i} of one of two original polygon configurations. Since this polygon configuration has homology ϵ in Σ, the homology class in $H_1(\Sigma_i, \partial\Sigma_i; \mathbb{Z}/2\mathbb{Z})$ of the restriction to Σ_i is $\Pi_i(\epsilon)$ by definition. As a consequence, the bichromatic edge configuration on Σ_i is a polygon configuration of $\mathcal{P}^{\Pi_i(\epsilon)}(G_{\Sigma_i})$. Moreover, since all edges in the bichromatic configuration are present twice, and since the weight of pairs of polygon configurations is the product of the edge-weights contained in the pair of configurations, the effective weight of a bichromatic edge e is squared and becomes:

$$\left(e^{-2J_{e^*}}\right)^2 = e^{-2(2J_{e^*})},$$

which corresponds to a doubling of the coupling constants.

- There are two spin configurations, denoted by $\pm\xi$, whose low-temperature expansion is P. Suppose that there exists a pair of spin configurations (σ, σ') whose low-temperature expansion has P as monochromatic edges, then $\sigma\sigma' = \pm\xi$. Let us assume $\sigma\sigma' = \xi$, the argument being similar in the other case, this has the effect of adding a global factor 2 when speaking of spin configurations. The relation $\sigma\sigma' = \xi$ implies that there is freedom of choice for exactly one spin configuration, say σ, the other being determined by their product ξ.

  Consider a connected component Σ_i, and a polygon configuration $P_i \in \mathcal{P}^{\Pi_i(\epsilon)}(G_{\Sigma_i})$. We want P_i to consist of doubled edges, so that in particular, it must contain all red edges. There are thus two choices for the first spin configuration of $G_{\Sigma_i}^*$, denoted by $\pm\sigma^i$. This holds for every $i \in \{1, \ldots, n_P\}$ and thus defines 2^{n_P} spin configurations $(\pm\sigma^1, \ldots, \pm\sigma^{n_P})$ of G^*. Recall that in each of the 2^{n_P} cases, the second spin configuration is determined by the condition $\sigma\sigma' = \xi$. Since on each connected component Σ_i, ξ is identically equal to ± 1, we deduce that $(\sigma')^i = \pm\sigma^i$. As a consequence, the low-temperature expansion of σ' exactly consists of edges of P_i, i.e., P_i consists of red and blue edges. Summarizing, there are $2 \cdot 2^{n_P}$ pairs of spin configurations, or 2^{n_P-1} pairs of polygon configurations $(P_{\text{red}}, P_{\text{blue}})$, such that monochromatic edges are those of P and bichromatic edges those of P_i, $i \in \{1, \ldots, n_P\}$. Note that by construction (choice of σ^i's), each polygon configuration $P_{\text{red}}, P_{\text{blue}}$ is in $\mathcal{P}^\epsilon(G)$.

$\square$

Consider a polygon configuration $P \in \mathcal{P}^0(G)$, and let $\epsilon \in H_1(\Sigma, \mathbb{Z}/2\mathbb{Z})$. Denote by $\mathcal{W}_{\text{d-Ising}}^\epsilon[\text{Mono} = P]$ the contribution of the set

$$\{(P_{\text{red}}, P_{\text{blue}}) \in \mathcal{P}^\epsilon(G) \times \mathcal{P}^\epsilon(G) : \text{Mono}(P_{\text{red}}, P_{\text{blue}}) = P\},$$

to the partition function $(Z_{\text{Ising}}^\epsilon(J))^2$, and by

$$\mathcal{W}_{\text{d-Ising}}[\text{Mono} = P] = \sum_{\epsilon \in H_1(\Sigma; \mathbb{Z}/2\mathbb{Z})} \mathcal{W}_{\text{d-Ising}}^\epsilon[\text{Mono} = P].$$

By the low-temperature expansion of the Ising partition function, the weight of each polygon configuration $P_{\text{red}}, P_{\text{blue}}$ is the product of edge-weights contained in the configuration. As a consequence, the contribution of $(P_{\text{red}}, P_{\text{blue}})$ can be decomposed as a product over monochromatic edges, and bichromatic edges of each of the components. Using Lemmas 3.1 and 3.2, this yields

Proposition 3.3. *For every polygon configuration $P \in \mathcal{P}^0(G)$ and every $\epsilon \in H_1(\Sigma, \mathbb{Z}/2\mathbb{Z})$,*

$$\mathcal{W}_{\text{d-Ising}}^\epsilon[\text{Mono} = P] = 2^{-1}\mathcal{C}\Big(\prod_{e \in P} e^{-2J_{e^*}}\Big)\Big(\prod_{i=1}^{n_P} 2Z_{\text{LT}}^{\Pi_i(\epsilon)}(G_{\Sigma_i}, 2J)\Big), \tag{3.1}$$

where $\mathcal{C} = \big(2\prod_{e \in E} e^{J_{e^*}}\big)^2$. Moreover, the double Ising partition function can be rewritten as:

$$Z_{\text{d-Ising}}(J) = \sum_{P \in \mathcal{P}^0(G)} \mathcal{W}_{\text{d-Ising}}[\text{Mono} = P],$$

and the probability measure $\mathbb{P}_{\text{d-Ising}}$ induces a probability measure on polygon configurations of $\mathcal{P}^0(G)$, given by:

$$\forall P \in \mathcal{P}^0(G), \quad \mathbb{P}_{\text{d-Ising}}[\text{Mono} = P] = \frac{\mathcal{W}_{\text{d-Ising}}[\text{Mono} = P]}{Z_{\text{d-Ising}}(J)}. \tag{3.2}$$

4 Mixed contour expansion

In [Nie84], Nienhuis rewrites the partition function of the Ashkin–Teller model on the square lattice as a statistical sum over polygon families on G and G^* which do not intersect. We apply the same approach to the double Ising model on Σ but some care is required to keep track of the homology class of the polygon configurations involved.

We fix $\epsilon \in H_1(\Sigma; \mathbb{Z}/2\mathbb{Z})$ and a polygon configuration $P \in \mathcal{P}^0(G)$. In Proposition 4.1, we apply the low/high-temperature duality to each of the terms $Z_{\mathrm{LT}}^{\Pi_i(\epsilon)}(G_{\Sigma_i}, 2J)$ involved in the expression of $\mathcal{W}_{\mathrm{d\text{-}Ising}}^\epsilon[\mathrm{Mono} = P]$ of Equation (3.1). This has the effect of transforming bichromatic polygon configurations of G_{Σ_i} into dual polygon configurations of $G_{\Sigma_i}^*$. Then, in Proposition 4.3, we sum over $\epsilon \in H_1(\Sigma; \mathbb{Z}/2\mathbb{Z})$, and show that the outcome simplifies to a sum over dual polygon configurations of the dual graph, having 0 homology class in $H_1(\Sigma; \mathbb{Z}/2\mathbb{Z})$, and not intersecting P.

Proposition 4.1. *For every polygon configuration $P \in \mathcal{P}^0(G)$ and every $\epsilon \in H_1(\Sigma, \mathbb{Z}/2\mathbb{Z})$,*

$$
\mathcal{W}_{\mathrm{d\text{-}Ising}}^\epsilon[\mathrm{Mono} = P] = \mathcal{C}'\Big(\prod_{e \in P} \frac{2e^{-2J_{e^*}}}{1 + e^{-4J_{e^*}}}\Big) \times
$$
$$
\times \prod_{i=1}^{n_P}\Big[\sum_{\tau^i \in H_1(\Sigma_i, \mathbb{Z}/2\mathbb{Z})} (-1)^{(\tau^i | \Pi_i(\epsilon))} \sum_{P_i^* \in \mathcal{P}^{\tau^i}(G_{\Sigma_i}^*)} \Big(\prod_{e^* \in P_i^*} \frac{1 - e^{-4J_{e^*}}}{1 + e^{-4J_{e^*}}}\Big)\Big],
$$

where, $\mathcal{C}' = 2^{|V^*|+1}\big(\prod_{e \in E} \cosh(2J_{e^*})\big).$

Proof. The expression for $\mathcal{W}_{\mathrm{d\text{-}Ising}}^\epsilon[\mathrm{Mono} = P]$ of Equation (3.1) can be rewritten as:

$$
\mathcal{W}_{\mathrm{d\text{-}Ising}}^\epsilon[\mathrm{Mono} = P] = 2^{n_P - 1}\mathcal{C}\big(\prod_{e \in P} e^{-2J_{e^*}}\big)\Big(\prod_{i=1}^{n_P} Z_{\mathrm{LT}}^{\Pi_i(\epsilon)}(G_{\Sigma_i}, 2J)\Big).
$$

For every $i \in \{1, \ldots, n_P\}$, the contribution, $Z_{\mathrm{LT}}^{\Pi_i(\epsilon)}(G_{\Sigma_i}, 2J)$ is the low-temperature expansion of an Ising model on vertices of $V_{\Sigma_i}^*$ with coupling constants $2J_{e^*}$ and defect condition $\Pi_i(\epsilon)$. Using the relation between Kramers and Wannier's low and high-temperature expansions of (2.5), it can be expressed as:

$$
Z_{\mathrm{LT}}^{\Pi_i(\epsilon)}(G_{\Sigma_i}, 2J) = \mathcal{A}_i \times \sum_{\tau^i \in H_1(\Sigma_i; \mathbb{Z}/2\mathbb{Z})} (-1)^{(\tau^i | \Pi_i(\epsilon))} Z_{\mathrm{HT}}^{\tau^i}(G_{\Sigma_i}, 2J),
$$

where

$$
\mathcal{A}_i = 2^{|V_{\Sigma_i}^*|-1} \prod_{e \in E_{\Sigma_i}} \frac{\cosh(2J_{e^*})}{e^{2J_{e^*}}}.
$$

Let us first compute the part which is independent of ϵ. Observing that the collection of sets of dual vertices $(V_{\Sigma_i}^*)_{i=1}^{n_P}$ is a partition of V^*, one writes:

$$
2^{n_P - 1}\mathcal{C}\big(\prod_{e \in P} e^{-2J_{e^*}}\big)\Big(\prod_{i=1}^{n_P} \mathcal{A}_i\Big) = 2^{n_P - 1}2^2\big(\prod_{e \in E} e^{2J_{e^*}}\big)\big(\prod_{e \in P} e^{-2J_{e^*}}\big)2^{|V^*|-n_P}\Big(\prod_{e \in E_{\Sigma_i}} \frac{\cosh(2J_{e^*})}{e^{2J_{e^*}}}\Big).
$$

Noticing that the collection of edges in the Σ_i's is exactly the set of edges of G not in P, we have:

$$
2^{n_P - 1}\mathcal{C}\big(\prod_{e \in P} e^{-2J_{e^*}}\big)\Big(\prod_{i=1}^{n_P} \mathcal{A}_i\Big) = 2^{|V^*|+1}\big(\prod_{e \in E} \cosh(2J_{e^*})\big)\big(\prod_{e \in P} \cosh(2J_{e^*})^{-1}\big).
$$

Define the constant $\mathcal{C}' = 2^{|V^*|+1}\left(\prod_{e \in E} \cosh(2J_{e^*})\right)$, then by definition of $Z_{\mathrm{HT}}^{\tau^i}(G_{\Sigma_i}, 2J)$, one deduces that $\mathcal{W}_{\mathrm{d\text{-}Ising}}^{\epsilon}[\mathrm{Mono} = P]$ equals:

$$\mathcal{C}'\Big(\prod_{e \in P} \cosh(2J_{e^*})^{-1}\Big) \prod_{i=1}^{n_P} \Big[\sum_{\tau^i \in H_1(\Sigma_i, \mathbb{Z}/2\mathbb{Z})} (-1)^{(\tau^i|\Pi_i(\epsilon))} \sum_{P_i^* \in \mathcal{P}^{\tau^i}(G_{\Sigma_i}^*)} \Big(\prod_{e^* \in P_i^*} \tanh(2J_{e^*}) \Big) \Big].$$

The proof of Proposition 4.1 is concluded by observing that

$$\cosh(2J_{e^*})^{-1} = \frac{2e^{-2J_{e^*}}}{1 + e^{-4J_{e^*}}}, \text{ and } \tanh(2J_{e^*}) = \frac{1 - e^{-4J_{e^*}}}{1 + e^{-4J_{e^*}}}. \qquad \square$$

In order to have an explicit expression for the contribution of P to the partition function $Z_{\mathrm{d\text{-}Ising}}(J)$, we need to sum the quantities $\mathcal{W}_{\mathrm{d\text{-}Ising}}^{\epsilon}[\mathrm{Mono} = P]$ of Proposition 4.1 over $\epsilon \in H_1(\Sigma; \mathbb{Z}/2\mathbb{Z})$. This is the object of the next proposition.

Proposition 4.2. *For every polygon configuration $P \in \mathcal{P}^0(G)$,*

$$\mathcal{W}_{\mathrm{d\text{-}Ising}}[\mathrm{Mono} = P] = \mathcal{C}_{\mathrm{I}} \Big(\prod_{e \in P} \frac{2e^{-2J_{e^*}}}{1 + e^{-4J_{e^*}}} \Big) \sum_{\{P^* \in \mathcal{P}^0(G^*): P \cap P^* = \emptyset\}} \Big(\prod_{e^* \in P^*} \frac{1 - e^{-4J_{e^*}}}{1 + e^{-4J_{e^*}}} \Big).$$

where $\mathcal{C}_{\mathrm{I}} = 2^{2g}\mathcal{C}' = 2^{|V^*|+2g+1} \left(\prod_{e \in E} \cosh(2J_{e^*}) \right).$

Proof. To simplify notation, let us write the product of weights of edges in polygon configurations as follows:

$$\Theta(P) = \prod_{e \in P} \frac{2e^{-2J_{e^*}}}{1 + e^{-4J_{e^*}}}, \quad \Theta^*(P_i^*) = \prod_{e^* \in P_i^*} \frac{1 - e^{-4J_{e^*}}}{1 + e^{-4J_{e^*}}}, \text{ for } i \in \{1, \ldots, n_P\}.$$

Then,

$$\mathcal{W}_{\mathrm{d\text{-}Ising}}[\mathrm{Mono} = P] = \mathcal{C}'\Theta(P) \sum_{\epsilon \in H_1(\Sigma; \mathbb{Z}/2\mathbb{Z})} \prod_{i=1}^{n_P} \Big[\sum_{\tau^i \in H_1(\Sigma_i, \mathbb{Z}/2\mathbb{Z})} (-1)^{(\tau^i|\Pi_i(\epsilon))} \sum_{P_i^* \in \mathcal{P}^{\tau^i}(G_{\Sigma_i}^*)} \Theta^*(P_i^*) \Big].$$

Expanding the product over $i \in \{1, \ldots, n_P\}$ and exchanging the summation over ϵ and $(\tau^1, \ldots, \tau^{n_P})$, one obtains that $\mathcal{W}_{\mathrm{d\text{-}Ising}}[\mathrm{Mono} = P]$ is equal to:

$$\mathcal{C}'\Theta(P) \sum_{(\tau^1, \ldots, \tau^{n_P}) \in \prod_{i=1}^{n_P} H_1(\Sigma_i, \mathbb{Z}/2\mathbb{Z})} \Big(\sum_{\epsilon \in H_1(\Sigma; \mathbb{Z}/2\mathbb{Z})} (-1)^{\sum_{i=1}^{n_P}(\tau^i|\Pi_i(\epsilon))} \Big) \prod_{i=1}^{n_P} \Big(\sum_{P_i^* \in \mathcal{P}^{\tau^i}(G_{\Sigma_i}^*)} \Theta^*(P_i^*) \Big).$$

The evaluation of the intersection form $(\tau^i|\Pi_i(\epsilon))$ on $H_1(\Sigma_i; \mathbb{Z}/2\mathbb{Z}) \times H_1(\Sigma_i, \partial\Sigma_i; \mathbb{Z}/2\mathbb{Z})$ is equal to $(\pi_i(\tau^i)|\epsilon)$ on $H_1(\Sigma; \mathbb{Z}/2\mathbb{Z}) \times H_1(\Sigma; \mathbb{Z}/2\mathbb{Z})$, where $\pi_i = \pi_{\Sigma, \Sigma_i}$ is the projection induced by the inclusion $\Sigma_i \subset \Sigma$, see Appendix A.6. Indeed, take a representative $\underline{\tau}^i$ of τ^i in Σ_i. Counting intersections with the restriction of a representative $\underline{\epsilon}$ of ϵ to Σ_i is the same as counting intersections with the whole $\underline{\epsilon}$, since $\underline{\tau}^i$ is confined to Σ_i and thus has no intersection with $\underline{\epsilon}$ outside of Σ_i. Therefore,

$$\sum_{i=1}^{n_P}(\tau^i|\Pi_i(\epsilon)) = \Big(\sum_{i=1}^{n_P} \pi_i(\tau^i) \Big| \epsilon \Big).$$

An application of the orthogonality relation (2.6) in the special case where $\partial\Sigma = \emptyset$ gives that the sum over ϵ is 0 unless $\sum_{i=1}^{n_P} \pi_i(\tau^i) = 0 \in H_1(\Sigma; \mathbb{Z}/2\mathbb{Z})$, *i.e.*, the homology class on the surface Σ of the whole dual polygon configuration $P^* = P_1^* \cup \cdots \cup P_{n_P}^*$ is zero, *i.e.*, $P^* \in \mathcal{P}^0(G^*)$, and that in this case, the sum over ϵ equals 2^{2g}. $\qquad \square$

As an interesting corollary, we obtain a mixed contour expansion for the partition function of the double Ising model, and the corresponding expression for the double Ising probability measure of monochromatic polygon configurations which, by Lemma 3.1, are the XOR polygon configurations.

Corollary 4.3.

- *The double Ising partition function can be rewritten as:*

$$Z_{\text{d-Ising}}(G^*, J) = \mathcal{C}_{\text{I}} \sum_{\{(P,P^*) \in \mathcal{P}^0(G) \times \mathcal{P}^0(G^*):\, P \cap P^* = \emptyset\}} \Big(\prod_{e \in P} \frac{2e^{-2J_{e^*}}}{1 + e^{-4J_{e^*}}} \Big) \Big(\prod_{e^* \in P^*} \frac{1 - e^{-4J_{e^*}}}{1 + e^{-4J_{e^*}}} \Big),$$

  where $\mathcal{C}_{\text{I}} = 2^{|V^*|+2g+1} \left(\prod_{e \in E} \cosh(2J_{e^*}) \right)$.
- *For every dual polygon configuration $P \in \mathcal{P}^0(G)$:*

$$\mathbb{P}_{\text{d-Ising}}[\text{XOR} = P] = \frac{\Big(\prod\limits_{e \in P} \frac{2e^{-2J_{e^*}}}{1 + e^{-4J_{e^*}}} \Big) \sum\limits_{\{P^* \in \mathcal{P}^0(G^*):\, P \cap P^* = \emptyset\}} \Big(\prod\limits_{e^* \in P^*} \frac{1 - e^{-4J_{e^*}}}{1 + e^{-4J_{e^*}}} \Big)}{\sum\limits_{\{(P,P^*) \in \mathcal{P}^0(G) \times \mathcal{P}^0(G^*):\, P \cap P^* = \emptyset\}} \Big(\prod\limits_{e \in P} \frac{2e^{-2J_{e^*}}}{1 + e^{-4J_{e^*}}} \Big) \Big(\prod\limits_{e^* \in P^*} \frac{1 - e^{-4J_{e^*}}}{1 + e^{-4J_{e^*}}} \Big)}.$$

Note that one can see Kramers and Wannier's duality on this expression: the duality relation between coupling constant

$$\tanh J^* = e^{-2J}$$

exchanges the expression for an edge of P and a dual edge of P^*.

5 Quadri-tilings and polygon configurations

In this section, we let G be a graph embedded in a compact, orientable, boundaryless surface Σ of genus g, and G^* denote its dual graph. For the moment, we forget about the double Ising model. The goal of this section is to explicitly construct pairs of non-intersecting polygon configurations of G and G^*, from a dimer model on a decorated, bipartite version G^{Q} of G, called *quadri-tilings* [dT07a].

This construction is done in two steps. The first step uses a mapping of Nienhuis [Nie84], which constructs pairs of non-intersecting primal and dual polygon configurations, from 6-vertex configurations of the medial graph; this is the subject of Section 5.1. The second step consists of using Wu–Lin/Dubédat's mapping [WL75, Dub11b] from the 6-vertex model of the medial graph to the bipartite dimer model on the decorated graph G^{Q}. This is the subject of Section 5.2.

Using the above results and those of Section 4, Theorem 5.5 proves that XOR loops of the double Ising model have the same law as primal polygon configurations of the bipartite dimer model.

5.1 6-vertex model and polygon configurations

The *medial graph* G^{M} of the graph G is defined as follows. Vertices of G^{M} correspond to edges of G. Two vertices of the medial graph are joined by an edge if the corresponding edges in the primal graph are incident. Observe that G^{M} is also the medial graph of the dual graph G^*, and that vertices of the medial graph all have degree four. Figure 3 represents the medial graph of a subset of $\mathbb{Z}^2$.

A *6V-configuration* or an *ice-type configuration* is an orientation of edges of G^{M}, such that every vertex has exactly two incoming edges [Lie67]. An equivalent way of
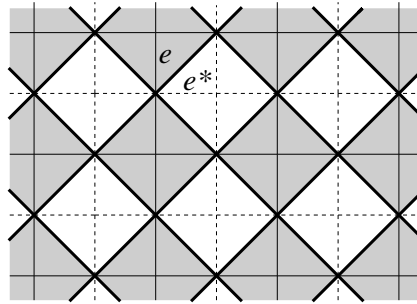
Figure 3: The medial graph of $\mathbb{Z}^2$: plain lines represent $\mathbb{Z}^2$, dotted lines represent the dual graph $\mathbb{Z}^2$, and thick plain lines represent the medial graph $(\mathbb{Z}^2)^M$. Grey (resp. white) faces of the medial graph correspond to primal (resp. dual) vertices of the initial graph.

defining 6-vertex configurations uses edge configurations instead of orientations, as represented in Figure 4. This approach is more useful in our context, so that we define a 6-*vertex configuration* to be an edge configuration, such that around every vertex of G^M, there is an even number of consecutive present edges.
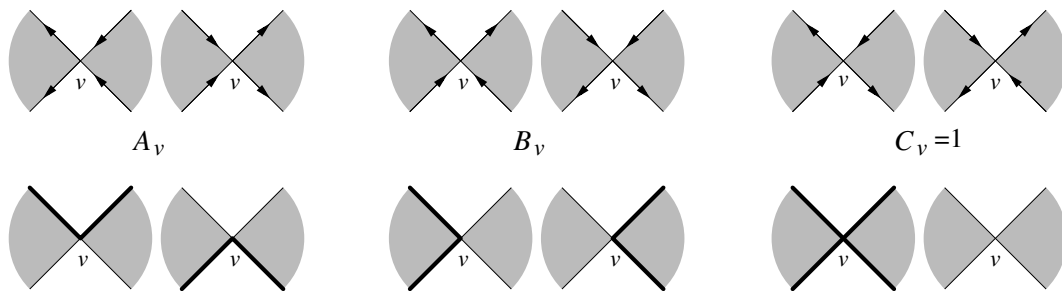

Figure 4: The six possible local configurations around a vertex v of the 6-vertex model, and their respective weights: arrow representation (top), and the even degree subgraph representation (bottom).

In order to make the 6-vertex model a model of statistical mechanics, weights are associated to local configurations around a vertex, and the probability of a 6-vertex configuration is taken to be proportional to the product of its local weights. In absence of external field, the weights of complementary local configurations are taken to be equal: there are thus three parameters for each vertex v of the medial graph G^M, denoted by A_v, B_v and C_v. Since multiplying these three parameters by the same positive constant does not change the measure, we set $C_v = 1$, see also Figure 4. Let us denote by $Z_{6\text{-vertex}}(G^M, (A, B))$ the partition function of this model.

Mapping I [Nie84]. Consider the following combinatorial mapping from 6-vertex configurations to edge configurations of the primal and dual graphs: whenever a vertex of G^M has two neighboring edges in the 6 vertex configuration, put the edge of G or G^* separating the present and the absent edges; see Figure 5. The following lemma characterizes this mapping, see also [Nie84].
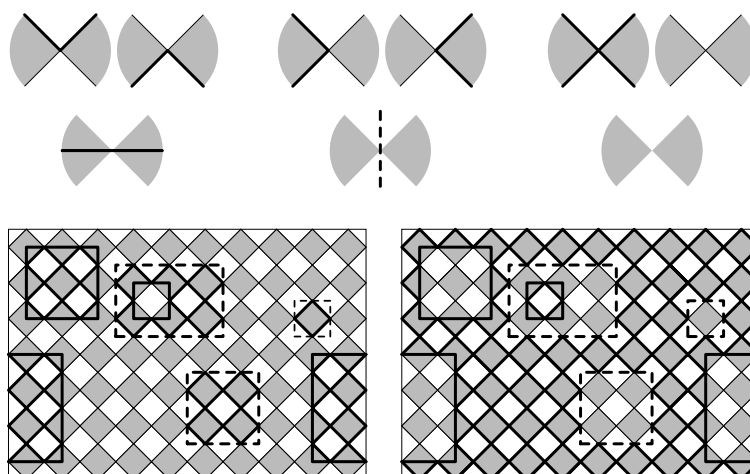
Lemma 5.1.

Figure 5: Mapping on the local level (top), and on the global level (bottom).

- *Mapping I associates to a 6-vertex configuration a pair of polygon configurations (P, P^*), which do not intersect and such that the homology class of $P \cup P^*$ in $H_1(\Sigma; \mathbb{Z}/2\mathbb{Z})$ is 0.*
- *Given a pair of polygon configurations (P, P^*) as above, there are exactly two 6-vertex configurations which are mapped to (P, P^*).*

Proof. A 6-vertex configuration consists of clusters of present/absent edges, see Figure 5. The primal/dual edge configuration assigned by the mapping consists of the boundary of those clusters. It is thus a polygon configuration with 0 homology class. A primal and the corresponding dual edge cannot intersect, since that would correspond to a configuration on G^{M} where around a vertex there is alternatively one edge present, one edge absent, then again one present, one absent, which is a forbidden local configuration for the 6-vertex model.

Conversely suppose we are given a pair of polygon configurations (P, P^*) as above. The fact that the homology class of $P \cup P^*$ in $H_1(\Sigma; \mathbb{Z}/2\mathbb{Z})$ is 0, exactly means that it is the boundary of domains that can be painted alternatively in two colors consistently. Put all edges of G^{M} in domains of one color, and remove all edges in domains of the other color. In this way, one exactly obtains two valid configurations of the 6-vertex model, one being the complement of the other, depending on which color is used to represent present edges, see also Figure 5. $\qquad\square$

Let us denote by $\mathcal{P}^0(G \cup G^*)$ the set of pairs (P, P^*) of polygon configurations of G and G^* respectively, such that the union $P \cup P^*$ has 0 homology class in $H_1(\Sigma; \mathbb{Z}/2\mathbb{Z})$.

Recall that to every edge e of the primal graph (resp. e^* of the dual graph), corresponds a vertex v of the medial graph, which we denote by $v(e)$ (resp. $v(e^*)$). Using this fact, one can naturally define a weight function on edges of G and G^*:

$$\forall e \in G, \quad a_e := A_{v(e)}; \quad \forall e^* \in G^*, \quad b_{e^*} := B_{v(e^*)}.$$

With this choice of weights and using Lemma 5.1, we obtain the following.

Lemma 5.2.

$$Z_{6\text{-vertex}}(G^{\mathrm{M}}, (A, B)) = 2 \sum_{\{(P, P^*) \in \mathcal{P}^0(G \cup G^*): \, P \cap P^* = \emptyset\}} \prod_{e \in P} a_e \prod_{e^* \in P^*} b_{e^*}.$$

5.2 Quadri-tilings and 6-vertex model

Let us define yet another graph built from the graph G. The *quadri-tiling* graph of G, denoted by G^{Q}, is the decorated graph obtained from G^{M} by replacing every vertex by a decoration which is a quadrangle. The graph G^{Q} is bipartite and can be drawn on the same surface as G. Edges shared by G^{Q} and G^{M} are referred to as *external* edges, and those inside the decorations as *internal*.
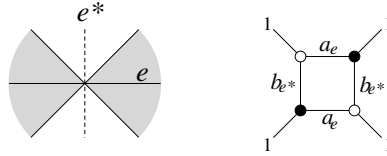
Figure 6: Decoration of a vertex of the medial graph G^{M} (left) to obtain a piece of the quadri-tiling graph G^{Q} (right).

A *dimer configuration* of G^{Q}, also known as a *perfect matching* is a spanning subgraph of G^{Q} where every vertex has degree exactly one. Let us denote by $\mathcal{M}(G^{\mathrm{Q}})$ the set of dimer configurations of the graph G^{Q}. In a particular decoration of G^{Q}, a dimer configuration of G looks like one of the seven possibilities represented in Figure 7 (top).

Assigning positive weights $(w_e)_{e \in E^{\mathrm{Q}}}$ to edges of G^{Q}, the *dimer Boltzmann measure*, denoted $\mathbb{P}_{\mathrm{Q}}$, is defined by:

$$\forall M \in \mathcal{M}(G^{\mathrm{Q}}), \quad \mathbb{P}_{\mathrm{Q}}(M) = \frac{\prod_{e \in M} w_e}{Z_{\mathrm{dimer}}(G^{\mathrm{Q}}, w)},$$

where $Z_{\mathrm{dimer}}(G^{\mathrm{Q}}, w) = \sum_{M \in \mathcal{M}(G^{\mathrm{Q}})} \prod_{e \in M} w_e$ is the dimer partition function. This defines a model of statistical mechanics, called the *dimer model* on G^{Q}.

Mapping II [WL75, Dub11b]. Requiring exterior edges to match yields a mapping from dimer configurations of G^{Q} to 6-vertex configurations of G^{M}; see Figure 7. This mapping between local configurations is one-to-one except in the empty edge case where this mapping is two-to-one.
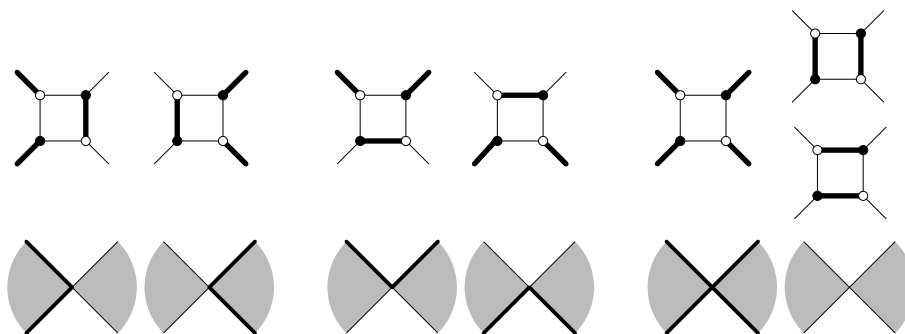

Figure 7: The local configurations of a quadri-tiling and the corresponding local 6-vertex configurations.

We now choose weights of edges in a specific way. Let A and B be positive functions on vertices of the medial graph G^{M}, defining weights of local 6-vertex configuration; and let a and b be the induced weight functions on edges of G and G^* respectively. The

weight function $w^{a,b}$ on edges of G^{Q} is defined as follows, see also Figure 6:

$$w_e^{a,b} = \begin{cases} 1 & \text{if } e \text{ is an external edge} \\ a_{\bar{e}} & \text{if } e \text{ is an interior edge, parallel to a primal edge } \bar{e} \\ b_{\bar{e}^*} & \text{if } e \text{ is an interior edge, parallel to a dual edge } \bar{e}^*. \end{cases}$$

Let us denote by $Z_{\mathrm{dimer}}(G^{\mathrm{Q}}, (A, B))$ the corresponding partition function. From now on, we suppose that local weights of the 6-vertex model satisfy the relation:

$$\forall v \in V(G^{\mathrm{M}}), \quad A_v^2 + B_v^2 = 1.$$

This implies that, $\forall v \in V(G^{\mathrm{M}})$, $\Delta_v = \frac{A_v^2 + B_v^2 - C_v^2}{2A_v B_v} = 0$, *i.e.*, the model is *free-fermionic*.

Using the weight functions a and b, the free-fermionic condition can be rewritten as:

$$\forall e \in E, \quad a_e^2 + b_{e^*}^2 = 1. \tag{5.1}$$

With this choice of weight, we thus obtain the following.

Lemma 5.3. *When local weights of the 6-vertex model satisfy the free-fermionic relation, Mapping II is weight preserving and,*

$$Z_{\mathrm{dimer}}(G^{\mathrm{Q}}, (A, B)) = Z_{6\text{-vertex}}(G^{\mathrm{M}}, (A, B)).$$

Let us now choose weights of edges of G^{Q} to depend on coupling constants (J_{e^*}) of the double Ising model:

$$\forall e \in E, \ a_e = \frac{2e^{-2J_{e^*}}}{1 + e^{-4J_{e^*}}}, \ \text{ and } \ \forall e^* \in E^*, \ b_{e^*} = \frac{1 - e^{-4J_{e^*}}}{1 + e^{-4J_{e^*}}}. \tag{5.2}$$

Then, it is straightforward to check that a and b satisfy the free-fermionic condition (5.1):

$$\forall e \in E, \ a_e^2 + b_{e^*}^2 = \frac{4e^{-4J_{e^*}} + (1 - e^{-4J_{e^*}})^2}{(1 + e^{-4J_{e^*}})^2} = 1.$$

It should be noted that in the more general case of the Ashkin–Teller model, when spins of the two Ising models interact, the mapping with the 6-vertex model still holds [Nie84, Sal87], but the model is not free-fermionic anymore.

Since weights a and b depend on coupling constants (J_{e^*}), we set J as argument for the corresponding dimer model partition function.

Recall that the mixed contour expansion of the double Ising partition function, see Corollary 4.3, involves pairs of non-intersecting primal and dual polygon configurations, each of which has 0 homology class in $H_1(\Sigma; \mathbb{Z}/2\mathbb{Z})$. We want to take the same restriction here.

Consider a dimer configuration M of the graph G^{Q}, then Mapping II assigns to M a 6-vertex configuration, and Mapping I assigns to this 6-vertex configuration a pair of non-intersecting polygon configuration of $\mathcal{P}^0(G \cup G^*)$. Let us denote this pair by $\mathrm{Poly}(M) = (\mathrm{Poly}_1(M), \mathrm{Poly}_2(M))$.

We restrict ourselves to dimer configurations M such that $\mathrm{Poly}_1(M)$ has 0 homology class, and denote by $\mathcal{M}^0(G^{\mathrm{Q}})$ this set. Note that since the superimposition $\mathrm{Poly}_1(M) \cup \mathrm{Poly}_2(M)$ has 0 homology class, this automatically implies that $\mathrm{Poly}_2(M)$ also has 0 homology. Let $\mathbb{P}_{\mathrm{Q}}^0$ be the corresponding dimer Boltzmann-measure, and $Z_{\mathrm{dimer}}^0(G^{\mathrm{Q}}, J)$ be the corresponding partition function.

Let $(P, P^*) \in \mathcal{P}^0(G) \times \mathcal{P}^0(G^*)$ such that $P \cap P^* = \emptyset$. Denote by $\mathcal{W}_{\mathrm{Q}}[\mathrm{Poly} = (P, P^*)]$ the contribution of the set:

$$\{M \in \mathcal{M}(G^{\mathrm{Q}}) : \mathrm{Poly}(M) = (P, P^*)\} \subset \mathcal{M}^0(G),$$

to the partition function $Z_{\mathrm{dimer}}^0(G^{\mathrm{Q}}, J)$. Then, as a consequence of Lemmas 5.2 and 5.3, we have:

Proposition 5.4. *When weights assigned to edges of the graph G^Q are chosen as in Equation (5.2), we have for all $(P, P^*) \in \mathcal{P}^0(G) \times \mathcal{P}^0(G^*)$, such that $P \cap P^* = \emptyset$:*

$$\mathcal{W}_Q[\text{Poly} = (P, P^*)] = 2\Big(\prod_{e \in P} \frac{2e^{-2J_{e^*}}}{1 + e^{-4J_{e^*}}}\Big)\Big(\prod_{e^* \in P^*} \frac{1 - e^{-4J_{e^*}}}{1 + e^{-4J_{e^*}}}\Big),$$

Moreover, the dimer model partition function can be written as:

$$Z^0_{\text{dimer}}(G^Q, J) = 2 \sum_{\{(P,P^*) \in \mathcal{P}^0(G) \times \mathcal{P}^0(G^*) : P \cap P^* = \emptyset\}} \Big(\prod_{e \in P} \frac{2e^{-2J_{e^*}}}{1 + e^{-4J_{e^*}}}\Big)\Big(\prod_{e^* \in P^*} \frac{1 - e^{-4J_{e^*}}}{1 + e^{-4J_{e^*}}}\Big)$$

and the probability measure $\mathbb{P}^0_Q$ induces a probability measure on polygon configurations of $\mathcal{P}^0(G)$, given by:

$$\mathbb{P}^0_Q[\text{Poly}_1 = P] = \frac{\Big(\prod_{e \in P} \frac{2e^{-2J_{e^*}}}{1+e^{-4J_{e^*}}}\Big) \sum_{\{P^* \in \mathcal{P}^0(G^*) : P \cap P^* = \emptyset\}} \Big(\prod_{e^* \in P^*} \frac{1-e^{-4J_{e^*}}}{1+e^{-4J_{e^*}}}\Big)}{\sum_{\{(P,P^*) \in \mathcal{P}^0(G) \times \mathcal{P}^0(G^*) : P \cap P^* = \emptyset\}} \Big(\prod_{e \in P} \frac{2e^{-2J_{e^*}}}{1+e^{-4J_{e^*}}}\Big)\Big(\prod_{e^* \in P^*} \frac{1-e^{-4J_{e^*}}}{1+e^{-4J_{e^*}}}\Big)}.$$

Combining Corollary 4.3 and Proposition 5.4 yields the following.

Theorem 5.5.

- *The double Ising partition function and the dimer model partition function are equal up to an explicit constant:*

$$Z_{\text{d-Ising}}(G^*, J) = 2^{|V^*|+2g}\Big(\prod_{e \in E} \cosh(2J_{e^*})\Big)Z^0_{\text{dimer}}(G^Q, J).$$

- *XOR-polygon configurations of the double Ising model on G^* have the same law as Poly_1 configurations of the corresponding dimer model on the bipartite graph G^Q:*

$$\forall P \in \mathcal{P}^0(G), \ \mathbb{P}_{\text{d-Ising}}[\text{XOR} = P] = \mathbb{P}^0_Q[\text{Poly}_1 = P].$$

Note that the first part of Theorem 5.5 can also be deduced from the results of [Dub11b] and [CDC13].

Since the quadri-tiling model is a bipartite dimer model, it can be studied in great detail using the tools of Kasteleyn theory, of which we recall some elements of in the next subsection. These tools can be used to study the distribution of the XOR Ising configurations.

5.3 Kasteleyn theory

We now recall some elements of the Kasteleyn theory for bipartite dimer models and apply it to the dimer model on G^Q. This simplified version for bipartite graphs of the more general theory developed by Temperley and Fisher, Kasteleyn [TF61, Kas67] is due to Percus [Per69]. The main tool is the *Kasteleyn matrix*, defined as follows in the bipartite case:

- rows (resp. columns) are indexed by white (resp. black) vertices;
- the absolute value of an entry is 0 if the corresponding white and black vertices are not adjacent, and is the dimer weight of the edge formed by these vertices when they are adjacent;
- signs of the entries are chosen in such a way that around all (bounded) faces, the number of minus signs around a face has the same parity as half of the degree of the face, minus 1.

If the graph G^{Q} is planar, the partition function of the model is, up to a global sign, the determinant of the Kasteleyn matrix. Indeed, when expanding the determinant of K as a sum over permutations, the only non-zero terms are those corresponding to dimer configurations, and their absolute value is the correct weight (see for example [Ken04] p.3). The third condition about signs is here to compensate the signatures of the permutations, so that all the terms exactly have the same sign. Kasteleyn showed [Kas61, Kas67] that such a choice of signs exists and is essentially unique: changing the sign of each edge around a particular vertex still yields a choice of signs satisfying the third condition, and one can pass from one valid choice to another by a succession of such operations. In order to get the right global sign, one can choose a reference dimer configuration M_0, giving a bijection between white and black vertices, agree that the order chosen for rows and columns of K is compatible with this bijection, and choose signs so that all entries of K corresponding to dimers of the reference configuration have sign $+$.

If the graph G^{Q} is embedded in a surface Σ of genus $g > 0$, the Kasteleyn theory is more complicated. There is a topological obstruction for the existence of a sign distribution on edges giving every dimer configuration a $+$ sign in the determinant expansion of a Kasteleyn matrix. There still exist choices of signs satisfying the third condition for a Kasteleyn matrix, but there is not just one, as in the planar case, but 2^{2g} classes of choices of signs, yielding 2^{2g} non-equivalent Kasteleyn matrices. From one of them, denoted by $K^{(0)}$, one can construct the other non-equivalent matrices denoted by $K^{(\epsilon)}$, $\epsilon \in H_1(\Sigma; \mathbb{Z}/2\mathbb{Z})$, by multiplying the sign of each edge crossing a representative of ϵ by -1.

In the expansion of the determinant of each of the 2^{2g} matrices, there are terms with different signs. The sign of a dimer configuration M is determined as follows. Let M_0 be a reference dimer configuration of G^{Q}. Consider the superimposition $M_0 \cup M$ of M_0 and of the dimer configuration M of G^{Q}. Each vertex of G^{Q} is incident to exactly two edges of the superimposition, so that we obtain a family of non-intersecting loops and doubled edges covering all vertices of G^{Q}. Loops of the superimposition also live on the surface Σ and may have non-trivial homology in $H_1(\Sigma; \mathbb{Z}/2\mathbb{Z})$. Given $\epsilon \in H_1(\Sigma; \mathbb{Z}/2\mathbb{Z})$, the sign of the dimer configuration M in the expansion of the determinant of $K^{(\epsilon)}$ depends on ϵ and the homology class in $\mathbb{Z}/2\mathbb{Z}$ of the loops of the superimposition $M_0 \cup M$. The determinant of the Kasteleyn matrix $K^{(\epsilon)}$ has thus the following form:

$$\det K^{(\epsilon)} = \sum_{\alpha \in H_1(\Sigma; \mathbb{Z}/2\mathbb{Z})} s_{\alpha,\epsilon} Z_{\mathrm{dimer}}^{(\alpha)},$$

where $Z_{\mathrm{dimer}}^{(\alpha)}$ is the partition function restricted to dimer configurations whose superimposition with M_0 has homology class α, and $s_{\alpha,\epsilon}$ is a sign depending only on ϵ and α.

The remarkable fact is that the linear relations between $\det K^{(\epsilon)}$ and $Z_{\mathrm{dimer}}^{(\alpha)}$ can be inverted explicitly and that each $Z_{\mathrm{dimer}}^{(\alpha)}$ can be written as a linear combination of the 2^{2g} determinants of Kasteleyn matrices [DZM$^+$96, GL99, Tes00, CR07, CR08]. Building on this result, Kenyon [Ken97] obtains an explicit expression for the dimer Boltzmann measure on dimer configurations of $Z_{\mathrm{dimer}}^{(\alpha)}$ involving the 2^{2g} Kasteleyn matrices and their inverses.

Let us return to the purpose of this paper. We are looking for an explicit expression for the law of XOR-polygon configurations of the double Ising model. By Theorem 5.5, this amounts to finding the law of dimer configurations M of G^{Q} such that $\mathrm{Poly}_1(M)$ has 0 homology class. The next lemma proves that by choosing the reference dimer configuration M_0 appropriately, the homology class of $\mathrm{Poly}_1(M)$ is equal to the homology class of the superimposition $M_0 \cup M$.

Lemma 5.6. *Let M_0 be the dimer configuration covering all internal edges of decorations parallel to dual edges of G^*, and let M be a dimer configuration of G^{Q}. Then, the homology classes of $M_0 \cup M$ and $\mathrm{Poly}_1(M)$ in $H_1(\Sigma; \mathbb{Z}/2\mathbb{Z})$ are equal.*

Proof. In order to prove that the homology classes are the same, it suffices to prove that they give the same result when computing the intersection form against any homology class $\tau \in H_1(\Sigma; \mathbb{Z}/2\mathbb{Z})$.

Let us fix such a class $\tau \in H_1(\Sigma; \mathbb{Z}/2\mathbb{Z})$. Let $\underline{\tau}$ be a representative of the class τ, realized as a path on G^*. We now show that the parity of the number of intersections between $\mathrm{Poly}_1(M)$ and $\underline{\tau}$, is equal to the number of intersections between $M \cup M_0$ and $\underline{\tau}$. All intersections occur in the interior of dual edge used by $\underline{\tau}$.

Fix e^* a dual edge used by $\underline{\tau}$. From the mappings above, the edge e belongs to $\mathrm{Poly}_1(M)$ if and only if the number of interior edges parallel to e in the corresponding rhombus covered by dimers in M is odd (see Figures 5 and 7). Since edges of M_0 are parallel to e^*, the parity of the number of intersections with e^* will be the same for $\mathrm{Poly}_1(M)$ as for $M \cup M_0$. Since this holds for every dual edge belonging to $\underline{\tau}$, it holds for $\underline{\tau}$. Therefore, the homology classes for $\mathrm{Poly}_1(M)$ and $M \cup M_0$ are the same. □

By Lemma 5.6, the restricted partition function $Z^{(\alpha)}_{\mathrm{dimer}}$ is also the partition function restricted to dimer configurations M such that $\mathrm{Poly}_1(M)$ has homology class α, this is in particular true for $\alpha = 0$. As a consequence, the Kasteleyn theory for dimer models defined on graphs embedded in surfaces of genus $g > 0$ described above, yields an explicit expression for the partition function and for the probability measure of XOR-polygon configurations of the double Ising model.

Note that classically, when studying dimer models one is interested in the full partition function $Z_{\mathrm{dimer}} = \sum_{\alpha \in H_1(\Sigma; \mathbb{Z}/2\mathbb{Z})} Z^{(\alpha)}_{\mathrm{dimer}}$, which from the above discussion is a linear combination of the determinants of the 2^{2g} Kasteleyn matrices. Since considering the restricted model where the homology class of dimer configurations is fixed is just a matter of considering another linear combination of determinants, results for the restricted model are readily obtained from those on the full model. This fact is used in the proof of Theorem 6.2.

This discussion of the relation of signs and homology considerations is not specific to the dimer model on G^{Q} but applies to any dimer model where the more general Kasteleyn theory applies, using *full* Kasteleyn matrices with rows and columns indexed by *all* vertices of the graph, and Pfaffians instead of determinants. We refer the reader to [CR07] for an intrinsic geometric interpretation of coefficients in the linear combination in this general context. The low-temperature polygon configurations of the Ising model can be mapped via Fisher's correspondence [Fis66] to a non-bipartite dimer model. Restricting the homology class of the polygon configurations can also be obtained on the dimer side with an appropriate linear combination of Pfaffians of Kasteleyn matrices.

6 The double Ising model at criticality on the whole plane

After having discussed in much generality the case of finite surfaces of genus g, we now want to consider the case of infinite planar graphs. From now on, we restrict ourselves to a special kind of graphs, the so-called *isoradial graphs*, with specific values of the coupling constants for the Ising model.

6.1 Isoradial graphs

Definition 6.1. *An* isoradial graph *[Duf68, Mer01, Ken02, KS05] is a planar graph G together with a proper embedding having the property that every bounded face is inscribed in a circle of fixed radius, which can be taken equal to 1.*

The regular square, triangular and hexagonal lattices with their standard embedding are isoradial. A fancier example is given in Figure 8 (left).
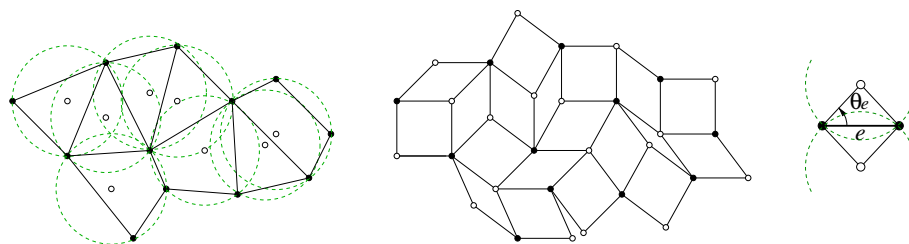

Figure 8: Left: an example of an isoradial graph. Middle: the corresponding rhombus graph. Right: the half-rhombus angle θ_e associated to an edge e.

The center of the circumscribing circle of a face can be identified with the corresponding dual vertex, implying that the dual of an isoradial graph is also isoradial.

The dual of the medial graph G^{M}, called the *diamond graph* of G and denoted by $G^{\diamond}$, has as set of vertices the union of those of G and G^*. There is an edge between $v \in V$ and $f^* \in V^*$ if and only if v is on the boundary of the face f corresponding to the dual vertex f^*; see Figure 8 (middle) for an example. Faces of $G^{\diamond}$ are rhombi with edge-length 1, diagonals of which correspond to an edge of G and its dual edge. To each edge e of G we can therefore associate a geometric angle $\theta_e \in (0, \pi/2)$, which is the half-angle of the rhombus containing e, measured between e and the edge of the rhombus; see Figure 8 (right). The family (θ_e) encodes the geometry of the embedding of the isoradial graph.

6.2 Statistical mechanics on isoradial graphs

When defining a statistical mechanical model on an isoradial graph, it is natural to relate statistical weights to the geometry of the embedding, and thus to choose the parameters attached to an edge (coupling constants for Ising, probability to be open for percolation, weight of an edge for dimer models, conductances for spanning trees or random walk,...) to be functions of the half-angle of that edge. For the Ising model, using discrete integrability considerations (invariance under star-triangle transformations), self-duality, the following expression for the interacting constants can be derived, see [Bax89]:

$$ J_e = J(\theta_e) = \frac{1}{2} \log \left(\frac{1 + \sin \theta_e}{\cos \theta_e} \right). $$

These are also known as *Yang–Baxter's coupling constants*.

This expression for J_e, when $\theta_e = \frac{\pi}{4}$, $\frac{\pi}{3}$ and $\frac{\pi}{6}$, coincides with the critical value of the square, hexagonal and triangular lattices respectively [KW41a, KW41b]. The Ising model with these coupling constants has been proved to be critical when the isoradial graph is bi-periodic [Li12, CDC13], we therefore refer to these values as *critical coupling constants*.

We suppose that the isoradial graph G is infinite, in the sense that the union of all rhombi of the diamond graph of G covers the whole plane.

Consider the corresponding bipartite dimer model on the infinite decorated quadri-tiling graph G^{Q}. Then, the correspondence for the weights described in Section 5.2, Equation (5.2) yields in this particular context:

$$ \forall e \in E, \ a_e = a(\theta_e) = \cos \theta_e, \quad \forall e^* \in E^*, \ b_{e^*} = b(\theta_{e^*}) = \cos \theta_{e^*} = \sin \theta_e. $$

Notice that with a particular embedding of the decoration, namely when external edges have length 0, and a and b edges form rectangles joining the mid-points of edges of each rhombus, the quadri-tiling graph G^Q is itself an isoradial graph with rhombi of edge-length $\frac{1}{2}$, and that weights (up to a global multiplicative factor of $\frac{1}{2}$) are those introduced by Kenyon [Ken02] to define critical dimer models on isoradial graphs.

It turns out that for the Ising and dimer models on infinite isoradial graphs with critical weights indicated above, it is possible to construct Gibbs probability measures [dT07a, BdT11], extending the Boltzmann probability measures in the DLR sense: conditional on the configuration of the model outside a given bounded region of the graph, the probability measure of a configuration inside the region is given by the Boltzmann probability measure defined by the weights above (and the proper boundary conditions). These measures have the wonderful property of *locality*: the probability of a local event only depends on the geometry of a neighborhood of the region where the event takes place, otherwise stated changing the isoradial graph outside of this region does not affect the probability.

We can therefore consider the critical Ising model (resp. dimer, in particular quadritilings models) on a general infinite isoradial graph, as being that particular Gibbs probability measures on Ising configurations (resp. dimers configurations) of that infinite graph.

We now work with a fixed infinite isoradial graph G. We denote by $\mathbb{P}^\infty_{\text{Ising}}$ the measure on configurations of the critical Ising model on G^*. By taking two independent copies of the critical Ising model on G^*, we get the Gibbs measure for the critical double Ising model $\mathbb{P}^\infty_{\text{d-Ising}} = \mathbb{P}^\infty_{\text{Ising}} \otimes \mathbb{P}^\infty_{\text{Ising}}$, from which XOR contours can be constructed, as in the finite case. We denote by $\mathbb{P}^\infty_Q$ the Gibbs measure on dimer configurations of the infinite graph G^Q.

6.3 Loops of the critical XOR Ising model on isoradial graphs

It turns out that the identity in law between polygon configurations of the critical XOR Ising model on G^* and those of the corresponding bipartite dimer model on G^Q remains true in the context of infinite isoradial graphs at criticality:

Theorem 6.2. *Let G be an infinite isoradial graph. The measure induced on polygon configurations of the critical XOR Ising model on G^*, and the measure induced on* primal contours *of the corresponding critical bipartite dimer model on G^Q have the same law: for any finite subset of edges $\mathcal{E} = \{e_1, \ldots, e_n\}$,*

$$\mathbb{P}^\infty_{\text{d-Ising}}[\mathcal{E} \subset \text{XOR}] = \mathbb{P}^\infty_Q[\mathcal{E} \subset \text{Poly}_1]. \tag{6.1}$$

Proof. Suppose first that the graph G is infinite and bi-periodic, invariant under the translation lattice Λ. Then the graph G^Q is also infinite and bi-periodic. The infinite volume Gibbs measure $\mathbb{P}^\infty_Q$ on dimer configurations of the bipartite graph G^Q is constructed in [KOS06] as the weak limit of the Boltzmann measures on the natural toroidal exhaustion $G^Q_n = G^Q/n\Lambda$ of the infinite bi-periodic graph G^Q. The infinite volume Gibbs measure $\mathbb{P}^\infty_{\text{Ising}}$ on low temperature Ising polygon configurations of G is constructed in [BdT10]. It uses Fisher's correspondence relating the low temperature expansion of the Ising model and the dimer model on a non-bipartite decorated version of the graph G. The construction then also consists in taking the weak limit of the dimer Boltzmann measures but, since the dimer graph is non-bipartite, more care is required in the proof of the convergence.

If we apply Theorem 5.5 to the specific case of the double Ising model on a toroidal, isoradial graph G^*_n with critical coupling constants, we know that on G_n, XOR polygon configurations have the same law as primal polygon configurations of the corresponding

bipartite dimer model on G_n^Q. The laws involved are the Boltzmann measures on configurations having restricted homology. But from Section 5.3, we know that restricting the homology amounts to taking other linear combinations of the Kasteleyn matrices and their inverses. This does neither change the proof of the convergence of the Boltzmann measures, nor the limit. Having equality in law for every n thus implies equality in the weak limit.

Suppose now that the graph G is infinite but not necessarily periodic. The infinite volume Gibbs measure $\mathbb{P}_Q^\infty$ of the critical dimer model on the bipartite graph G^Q is constructed in [dT07a]. The construction has two main ingredients: the *locality property* meaning that the probability of a local event only depends on the geometry of the embedding of G^Q in a bounded domain containing edges involved in the event, and Theorem 5 of [dT07a] which states that any simply connected subgraph of an infinite rhombus graph can be embedded in a periodic rhombus graph. The infinite volume Gibbs measure $\mathbb{P}_{\mathrm{Ising}}^\infty$ of the low temperature representation of the critical Ising model on G is constructed in [BdT11] using the same argument. This implies that one can identify the probability of local events on a non-periodic graph G with the one of a periodic graph having a fundamental domain coinciding with G on a ball sufficiently large to contain a neighborhood of the region of the graph involved in the event. As a consequence, equality in law still holds in the non-periodic case. □

7 Height function on quadri-tilings

Dimer configurations of the quadri-tiling graph G^Q, like all bipartite planar dimer models, can be interpreted as random surfaces, via a *height function*. It is the main ingredient to relate the previous results connecting XOR loops and dimers with Wilson's conjecture.

7.1 Definition and properties of the height function

Let us now recall the definition of height function, used in [dT07a]. A dimer configuration M of a planar bipartite graph can be interpreted as a unit flow α_M, flowing by 1 along each matched edge of M, from the white vertex to the black one. It is a function on edges having divergence $+1$ at each white vertex and -1 at each black vertex. Subtracting from α_M another flow with the same divergence at every vertex, yields a divergence-free flow, whose dual is the differential of a function on faces of this graph.

There is a natural candidate for this unit reference flow: since in a dimer configuration there is exactly one dimer incident to every vertex, the sum over all edges incident to any given vertex of the probability that this edge is covered by a dimer, is equal to 1. This means that the flow α_0, flowing by $\mathbb{P}_Q^\infty(e)^1$ from the white vertex to the black one along each edge e of the graph, is a flow with divergence $+1$ (resp. -1) at every white (resp. black) vertex.

The height function h on quadri-tilings is defined as follows. For every dimer configuration M of G^Q, h^M is a function on faces of G^Q, such that for every pair of neighboring faces f and f' of G^Q sharing an edge e, with the additional property that when traversing e from f to f', the black vertex of e is on the left:

$$h^M(f') - h^M(f) = \alpha_M(e) - \alpha_0(e).$$

When faces f and f' are not incident, choose a path $f = f_0, f_1, \ldots, f_n = f'$ in the

---

[1]The graph G^Q is isoradial and infinite, and the weights for the quadri-tilings are critical. So in this particular context, we know [Ken02] that the probability of an edge is given by θ/π, where θ is the half-angle of the rhombus containing that edge.

dual graph joining f and f', then:

$$h^M(f') - h^M(f) = \sum_{i=0}^{n-1}(h^M(f_{i+1}) - h^M(f_i)).$$

This definition is consistent, *i.e.*, independent of the choice of path from f to f', because the flow $\alpha_M - \alpha_0$ is divergence free; it determines h^M up to a global additive constant, which can be fixed by saying that the height at a particular given face of G^Q is 0. Faces of G^Q are split into three distinct subsets, those corresponding to: vertices of G, vertices of the dual G^* and edges of G (or G^*). We suppose for the sake of definiteness that the face where the height is fixed at 0 corresponds to some particular vertex of G.

Denote by h_V^M (resp. $h_{V^*}^M$) the restriction of h^M to vertices of G (resp. to vertices of G^*).

The next lemma describes possible height changes between pairs of vertices of the primal (resp. dual) graph, incident in the primal (resp. dual) graph. To simplify the picture, we consider primal and dual vertices to be around a rhombus of the diamond graph; see Figure 9.
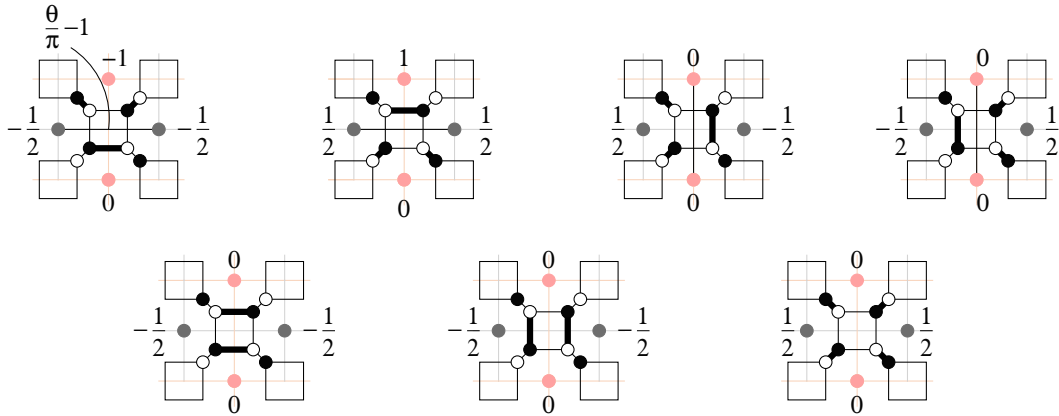

Figure 9: Height changes for the dimer model in a rhombus of the diamond graph.

Lemma 7.1.

- *The function h_V^M (resp. $h_{V^*}^M$) takes values in $\mathbb{Z}$ (resp. $\mathbb{Z} + \frac{1}{2}$).*
- *The increment of h_V^M (resp. $h_{V^*}^M$) between two neighboring vertices of G (resp. of G^*) is -1, 0, or 1.*
- *The increment of h_V^M (resp. $h_{V^*}^M$) is non-zero if and only if the two vertices are separated by an edge of $\mathrm{Poly}_2(M)$ (resp. $\mathrm{Poly}_1(M)$).*

Proof. Let e_1, e_2 be two interior edges of G^Q, parallel to an edge of G, as in Figure 9. Then, the reference flow α_0 has the same value but opposite direction on these two edges. As a consequence, using the definition of the height function,

$$h^M(v_2^*) - h^M(v_1^*) = \mathbb{I}_{e_1}(M) - \mathbb{P}_Q^\infty(e_1) - \mathbb{I}_{e_2}(M) + \mathbb{P}_Q^\infty(e_1) = \mathbb{I}_{e_1}(M) - \mathbb{I}_{e_2}(M).$$

A similar expression holds for $h^M(v_2) - h^M(v_1)$. This proves that the increment of h^M between two neighboring vertices of G (resp. G^*) is equal to -1, 0, or 1. Because of our convention for the base point, this implies that h^M takes integer values on G. To see that h^M takes half-integer values on G^*, one just has to notice that the reference flow α_0 separating two vertices v (on G) and v^* (on G^*) which are neighbors on $G^\diamond$ is $\frac{\pi/2}{\pi} = \frac{1}{2}$ since the corresponding rhombus in the isoradial graph G^Q is flat. $\qquad\square$

Remark 7.2. *Note that another choice of reference unit flow is the one coming from the reference dimer configuration M_0, where a white-to-black unit is flowing along all interior edges parallel to edges of G^*. This produces a random height function whose restriction to vertices of G, resp. of G^*, coincides with h_V, resp. h_{V^*} (up to an additive constant).*

Remark 7.3. *The height function h^M on $V \cup V^*$ can be defined directly from the 6-vertex dimer configuration, using the representation in terms of orientations depicted in Figure 4. Since the number of incoming and outgoing edges is the same at each vertex, the set of edges in the 6-vertex configuration can be partitioned into oriented contours. These contours are the level lines of the restriction of h^M to $V \cup V^*$ separating two successive half-integer values, and can thus be used to reconstruct h^M.*

The *level lines* of h_V (resp. h_{V^*}) are the set of closed contours on G^* (on resp G) separating clusters of vertices of G (resp. of G^*) where h_V (resp. h_{V^*}) takes the same value.

Returning to the definition of the pair of polygon configurations $\text{Poly}(M)$ assigned to a quadri-tiling M, we immediately obtain the following:

Lemma 7.4. *Let M be a dimer configuration of G^Q, then level lines of h_V^M, respectively $h_{V^*}^M$, exactly correspond to the polygon configuration $\text{Poly}_1(M)$, respectively $\text{Poly}_2(M)$.*

Note that due to the fact that $\text{Poly}_1(M)$ and $\text{Poly}_2(M)$ do not cross, the increments of h^M along two diagonals of a rhombus cannot be both non-zero. As a consequence, on contour lines of h_V^M, $h_{V^*}^M$ is constant.

Combining Lemma 7.4 with Theorem 6.2 stating that monochromatic polygon configurations of the XOR Ising model have the same distribution as primal polygon configurations of dimer configurations of G^Q, we obtain one of the main theorems of this paper:

Theorem 7.5. *Monochromatic polygon configurations of the critical XOR-Ising model have the same distribution as level lines of the restriction to primal vertices of the height function of dimer configurations of G^Q.*

7.2 Wilson's conjecture

In [Wil11], Wilson presented extensive numerical simulations on loops of the critical XOR Ising model on the honeycomb lattice, on the base of which he conjectured the following:

Conjecture 7.6 (Wilson [Wil11])**.** *The scaling limit of the family of loops of the critical XOR Ising model are the level lines of the Gaussian free field corresponding to levels that are odd multiples of $\frac{\sqrt{\pi}}{2}$.*

The Gaussian free field is a wild object: it is a random *generalized* function, and not a function, and as such, there is no direct way to define what its level lines are. The level lines of the Gaussian free field are understood here as the scaling limit when the mesh goes to zero of the level lines of the discrete Gaussian free field on a triangulation of the domain, which separate domains where the field is above or below a certain level [SS09].

The level lines of the Gaussian free field corresponding to levels that are odd multiples of $\lambda = \sqrt{\frac{\pi}{8}}$ form a CLE_4 [SS09, MS]. The contour lines of the XOR Ising models are thus conjectured to have the same limiting behavior as the CLE_4, except that there are a factor of $\sqrt{2}$ times fewer loops in the XOR Ising picture. This conjecture is in agreement with predictions of conformal field theory [IR11, PS11].

Theorem 7.5 can be interpreted as a proof of a version of Wilson's conjecture in a discrete setting, before passing to the scaling limit, and brings some elements for the complete proof of this conjecture. In particular, it explains the link with the Gaussian free field and the factor $\sqrt{2}$, as we will now show.

For $\varepsilon > 0$, denote by $G^{\mathrm{Q}}_\varepsilon$ the embedding of G^{Q} in the plane where rhombi of G^{Q} have side length ε. For every dual vertex v in $G^{\mathrm{Q}*}$, define v^ε the vertex in $G^{\mathrm{Q}*}_\varepsilon$ corresponding to the dual vertex v.

The random height function h can be interpreted on $G^{\mathrm{Q}}_\varepsilon$ as a *random distribution* [GV77], *i.e.*, a continuous random linear form on the set $\mathcal{C}^\infty_{0,c}(\mathbb{R}^2)$ of compactly supported smooth, zero mean functions, denoted by H^ε: for every $\varphi \in \mathcal{C}^\infty_{0,c}(\mathbb{R}^2)$,

$$H^\varepsilon(\varphi) = \sum_{v \in G^{\mathrm{Q}*}} \mathrm{area}(v^\varepsilon) h(v) \varphi(v^\varepsilon),$$

where $\mathrm{area}(v^\varepsilon) = \varepsilon^2 \mathrm{area}(v)$ is the area of the face of $G^{\mathrm{Q}}_\varepsilon$ associated to v^ε.

In [dT07b], the second author proved the following convergence result for the height function of the dimer model on G^{Q}:

Theorem 7.7 ([dT07b]). *As ε goes to 0, the height function on the critical quadri-tilings, as a random distribution, converges in law to $\frac{1}{\sqrt{\pi}}$ times the Gaussian free field.*

The result also holds for the restriction of h to G (resp. to G^*) as soon as $\mathrm{area}(v)$ is replaced by the area of the corresponding face of G (resp. G^*).

As contour lines of the restriction of h to G separate integer values, they can be understood as discrete level lines corresponding to half-integer values. Therefore, it is natural to expect that these contour lines converge to the contour lines of the limiting object, *i.e.*, to level lines for the Gaussian free field with levels $(k + \frac{1}{2})\sqrt{\pi}$, $k \in \mathbb{Z}$, which would prove Wilson's conjecture. Unfortunately, the result for the convergence result of the height function to the Gaussian free field is too weak to ensure convergence of contour lines.

The convergence result in the paper [dT07b] applies not only to critical quadri-tilings, but to all bipartite planar dimer models on isoradial graphs with critical weights. It is conjectured that the family of loops obtained by superimposing two independent critical dimer configurations converges to CLE_4. This is supported by the fact that each of the dimer configurations can be described by a height function, converging in the scaling limit to $1/\sqrt{\pi}$ times the Gaussian Free Field, the two fields being independent. Dimer loops are the half integer level lines of the difference, which by independence converges (in a weak sense) to $\sqrt{2/\pi}$ times the Gaussian free field, and it is known that level lines $(k + 1/2)\sqrt{\frac{\pi}{2}}$ of the Gaussian free field are a CLE_4.

Therefore, the factor $\sqrt{2}$ in Wilson's conjecture corresponds to the fact that contours in the XOR Ising model have to do with contour lines of only one dimer height function, as opposed to two for dimer loops.

A Some elements of homology theory on surfaces

Here are some general facts about homology theory on surfaces which are useful in the context of this paper. More details can be found in the references [Ful95, Mau96, Mas91]. We consider Σ to be a compact, orientable surface of genus g with boundary $\partial\Sigma$ consisting of p components. The boundary may be empty, in which case $p = 0$.

We are interested in the *first* homology group H_1, and in the case where the target abelian group is $\mathbb{Z}/2\mathbb{Z}$. The other non-trivial homology groups H_0 and H_2 are isomorphic to $\mathbb{Z}/2\mathbb{Z}$, when Σ is connected.

A.1 1-chains and first homology group

A 1-*chain* is a formal linear combination of 1-dimensional submanifolds of Σ. The coefficients here will be taken to be in $\mathbb{Z}/2\mathbb{Z}$. The space of 1-chains with coefficients in $\mathbb{Z}/2\mathbb{Z}$ is a $\mathbb{Z}/2\mathbb{Z}$-vector space. Note that since the target group is $\mathbb{Z}/2\mathbb{Z}$, we do not need to care about orientations of 1-chains, and the sum is the same as the difference. If two 1-chains are the sums of pairwise disjoint submanifolds

$$\gamma = \sum_{c \in A} c, \quad \gamma' = \sum_{c \in A'} c,$$

with $c \neq c' \Rightarrow c \cap c' = \emptyset$, then

$$\gamma + \gamma' = \sum_{c \in A \cup A'} c,$$

so that we can think morally of the addition as the union for disjoint 1-chains.

The boundary of a 1-chain is the formal linear combination of the end points of the 1-dimensional submanifolds it consists of. A 1-chain is a *cycle* if its boundary is empty. An equivalence relation on the space of cycles is defined as follows: two cycles γ and γ' are equivalent if their sum is the boundary of a 2-dimensional submanifold of Σ. Note that a connected component of the boundary of a 2-dimensional submanifold of Σ may be not itself the whole boundary of a submanifold, and as such may not be equivalent to the empty chain for the relation above. The *first homology group* $H_1(\Sigma; \mathbb{Z}/2\mathbb{Z})$ is the set of equivalence classes for this relation. It has a structure of $\mathbb{Z}/2\mathbb{Z}$-vector space inherited from the one of the space of 1-chains.

A.2 Relative homology

If A is a closed subset of Σ, then one can also consider *homology relative to A*. As above, one defines a notion of cycle and boundary, relative to A this time: a *relative cycle* is a 1-chain whose boundary is in A. A *relative boundary* is a 1-chain in Σ for which there exists a 1-chain in A, such that the sum of the two is a boundary in Σ. Associated to this concept is an equivalence relation on relative cycles: two relative cycles are equivalent if their sum is a relative boundary. Then, the *first homology group relative to A*, denoted by $H_1(\Sigma, A; \mathbb{Z}/2\mathbb{Z})$, is the $\mathbb{Z}/2\mathbb{Z}$-vector space generated by relative cycles, quotiented by this equivalence relation.

A particular example of interest is when $A = \partial \Sigma$. Representatives of equivalence classes of $H_1(\Sigma, \partial \Sigma; \mathbb{Z}/2\mathbb{Z})$ are finite unions of cycles and paths attached to components of the boundary.

Note that when $\partial \Sigma$ is empty, the homology of Σ relative to its boundary coincides with the usual homology.

A.3 Explicit bases of homology

The two homology groups $H_1(\Sigma; \mathbb{Z}/2\mathbb{Z})$ and $H_1(\Sigma, \partial \Sigma; \mathbb{Z}/2\mathbb{Z})$ turn out to have the same dimension

$$N = \begin{cases} 2g & \text{if } p = 0 \text{ or } 1, \\ 2g + p - 1 & \text{otherwise.} \end{cases}$$

For each of the groups, a basis can be explicitly given. Label the handles of Σ from 1 to g, and the p components of the boundary from C_0 to C_{p-1}. For $H_1(\Sigma; \mathbb{Z}/2\mathbb{Z})$, choose N cycles $(\underline{\lambda}_i)_{i=1}^N$ on Σ, as follows:

- for $i \in \{1, \ldots, g\}$, take $\underline{\lambda}_{2i-1}$ and $\underline{\lambda}_{2i}$ to be winding around the i-th handle in two transverse directions,

- for $i \in \{1, \ldots, N - 2g\}$, take $\underline{\lambda}_{2g+i}$ to be winding around C_i, without crossing $\underline{\lambda}_1, \ldots, \underline{\lambda}_{2g}$.

Denote by λ_i the homology class of $\underline{\lambda}_i$. Then, the collection $(\lambda_i)_{i=1}^N$ is a basis of $H_1(\Sigma; \mathbb{Z}/2\mathbb{Z})$: any 1-chain on Σ has the same homology class as a sum of λ_i's. The first homology group $H_1(\Sigma; \mathbb{Z}/2\mathbb{Z})$ is isomorphic to $(\mathbb{Z}/2\mathbb{Z})^N$: for every $i \in \{1, \ldots, N\}$, the basis element λ_i is mapped to the basis element of $(\mathbb{Z}/2\mathbb{Z})^N$ consisting of 0's and a 1 at position i.

For $H_1(\Sigma, \partial\Sigma; \mathbb{Z}/2\mathbb{Z})$, choose N cycles $(\underline{\gamma}_i)_{i=1}^N$ on Σ, as follows:

- for $i \in \{1, \ldots, g\}$, take $\underline{\gamma}_{2i-1} = \underline{\lambda}_{2i}$, and $\underline{\gamma}_{2i} = \underline{\lambda}_{2i-1}$,
- for $i \in \{1, \ldots, N - 2g\}$, take $\underline{\gamma}_{2g+i}$ to be a path from C_0 to C_i.

Denote by γ_i the relative homology class of $\underline{\gamma}_i$. Then, the collection $(\gamma_i)_{i=1}^N$ is a basis for $H_1(\Sigma, \partial\Sigma; \mathbb{Z}/2\mathbb{Z})$. The group $H_1(\Sigma, \partial\Sigma; \mathbb{Z}/2\mathbb{Z})$ is also isomorphic to $(\mathbb{Z}/2\mathbb{Z})^N$. The two bases $(\lambda_i)_{i=1}^N$ and $(\gamma_i)_{i=1}^N$ are dual to each other as explained in Appendix A.5.

A.4 Representatives of homology classes on graphs

Consider a cellular decomposition of the surface Σ by a graph G_Σ, as in Section 2. The embedding of G_Σ on Σ defines a notion of dual graph for G_Σ, denoted by G_Σ^*. Then representatives of any homology class of $H_1(\Sigma; \mathbb{Z}/2\mathbb{Z})$ (resp. any relative homology class of $H_1(\Sigma, \partial\Sigma; \mathbb{Z}/2\mathbb{Z})$) can be realized as combinatorial paths on G^* (resp. G). Figure 10 provides an example of representatives of the bases $(\lambda_i)_{i=1}^N$ and $(\gamma_i)_{i=1}^N$ defined in Section A.3.
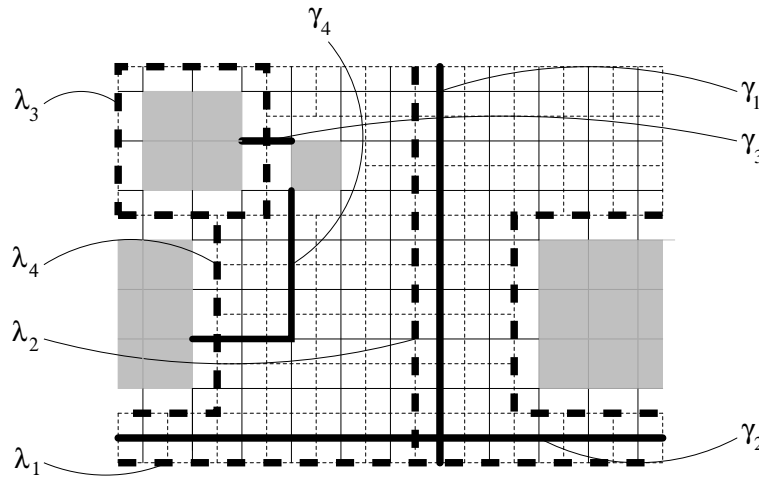

Figure 10: Representatives of a basis $(\lambda_i)_{i=1}^4$ of $H_1(\Sigma; \mathbb{Z}/2\mathbb{Z})$ (dotted lines), and of a basis $(\gamma_i)_{i=1}^4$ of $H_1(\Sigma, \partial\Sigma; \mathbb{Z}/2\mathbb{Z})$ (plain lines).

A.5 Intersection form

There is a natural pairing between $H_1(\Sigma; \mathbb{Z}/2\mathbb{Z})$ and $H_1(\Sigma, \partial\Sigma; \mathbb{Z}/2\mathbb{Z})$, called the *intersection form*:

$$(\cdot|\cdot) : H_1(\Sigma; \mathbb{Z}/2\mathbb{Z}) \times H_1(\Sigma, \partial\Sigma; \mathbb{Z}/2\mathbb{Z}) \longrightarrow \mathbb{Z}/2\mathbb{Z},$$

defined as follows. Let $\tau \in H_1(\Sigma; \mathbb{Z}/2\mathbb{Z})$ and $\epsilon \in H_1(\Sigma, \partial\Sigma; \mathbb{Z}/2\mathbb{Z})$ be two homology classes. Take representatives $\underline{\tau}$ and $\underline{\epsilon}$ for two classes τ and ϵ respectively. Then $(\tau|\epsilon)$ is

defined as the parity of the number of intersections of $\underline{\tau}$ and $\underline{\epsilon}$. This definition does not depend on the choice of representatives.

In the explicit bases of $H_1(\Sigma; \mathbb{Z}/2\mathbb{Z})$ and $H_1(\Sigma, \partial\Sigma; \mathbb{Z}/2\mathbb{Z})$ chosen in Appendix A.3, the matrix of the intersection form is the identity. The pairing is thus non-degenerate and defines an isomorphism between $H_1(\Sigma; \mathbb{Z}/2\mathbb{Z})$ and $H_1(\Sigma, \partial\Sigma; \mathbb{Z}/2\mathbb{Z})$. This is an explicit realization of the Poincaré–Lefschetz duality; see Theorem 5.4.13 and Corollary 5.2.12 in [Mau96].

A.6 Inclusion, excision and morphisms for homology

Suppose that there exists a larger surface $\tilde{\Sigma}$ containing Σ. Then a 1-chain in Σ is in particular a chain in $\tilde{\Sigma}$, and a boundary in Σ is in particular a boundary in $\tilde{\Sigma}$. This implies that the inclusion $\Sigma \subset \tilde{\Sigma}$ induces a morphism

$$\pi_{\tilde{\Sigma}, \Sigma} : H_1(\Sigma; \mathbb{Z}/2\mathbb{Z}) \longrightarrow H_1(\tilde{\Sigma}; \mathbb{Z}/2\mathbb{Z}).$$

The inclusion also induces morphisms for relative homology groups: if the subset $A \subset \Sigma$ is included in a subset $B \subset \tilde{\Sigma}$, then any relative chain (resp. cycle) in Σ relative to A is in particular a relative chain (resp. cycle) in $\tilde{\Sigma}$ relative to B (just by forgetting what is in $B \setminus A$). Therefore, this induces a morphism

$$H_1(\Sigma, A; \mathbb{Z}/2\mathbb{Z}) \longrightarrow H_1(\tilde{\Sigma}, B; \mathbb{Z}/2\mathbb{Z}),$$

giving the homology class in $\tilde{\Sigma}$ relative to B of the restriction to $\tilde{\Sigma} \setminus B$ of any representative of an element of $H_1(\Sigma, A; \mathbb{Z}/2\mathbb{Z})$. In the special case when $\Sigma = \tilde{\Sigma}$ and A is empty, we get the application $\iota_{\tilde{\Sigma}, B}$:

$$\iota_{\tilde{\Sigma}, B} = H_1(\tilde{\Sigma}; \mathbb{Z}/2\mathbb{Z}) \longrightarrow H_1(\tilde{\Sigma}, B; \mathbb{Z}/2\mathbb{Z}).$$

Moreover, the *excision theorem* ([Mau96], Theorem 8.2.1) states that if we cut out an open set U from both $\tilde{\Sigma}$ and B, the relative homology groups $H_1(\tilde{\Sigma}, B; \mathbb{Z}/2\mathbb{Z})$ and $H_1(\tilde{\Sigma} \setminus U, B \setminus U; \mathbb{Z}/2\mathbb{Z})$ are isomorphic. In particular, when $U = \Sigma^c = \tilde{\Sigma} \setminus \Sigma$ and $B = \overline{U}$, then the excision theorem states that $H_1(\tilde{\Sigma}, \Sigma^c; \mathbb{Z}/2\mathbb{Z})$ and $H_1(\Sigma, \partial\Sigma; \mathbb{Z}/2\mathbb{Z})$ are isomorphic. Let $e_{\tilde{\Sigma}, \Sigma}$ the isomorphism from the former space to latter. The composition $\Pi_{\tilde{\Sigma}, \Sigma} = e_{\tilde{\Sigma}, \Sigma} \circ \iota_{\tilde{\Sigma}, B}$ defines a morphism from $H_1(\tilde{\Sigma}; \mathbb{Z}/2\mathbb{Z})$ to $H_1(\Sigma, \partial\Sigma; \mathbb{Z}/2\mathbb{Z})$.

To construct a representative of $\Pi_{\tilde{\Sigma}, \Sigma}(\epsilon)$ for a homology class $\epsilon \in H_1(\tilde{\Sigma}; \mathbb{Z}/2\mathbb{Z})$, consider $\underline{\epsilon}$ a cycle representing ϵ in $\tilde{\Sigma}$. A representative of $\Pi_{\tilde{\Sigma}, \Sigma}(\epsilon)$ is then simply obtained by taking the intersection of $\underline{\epsilon}$ with Σ, which is a relative 1-chain of Σ relative to its boundary $\partial\Sigma$.

References

[AT43] J. Ashkin and E. Teller. Statistics of two-dimensional lattices with four components. *Phys. Rev.*, 64:178–184, Sep 1943.

[Bax89] R. J. Baxter. *Exactly solved models in statistical mechanics*. Academic Press Inc. [Harcourt Brace Jovanovich Publishers], London, 1989. Reprint of the 1982 original. MR-0998375

[BdT10] C. Boutillier and B. de Tilière. The critical Z-invariant Ising model via dimers: the periodic case. *Probab. theory and related fields*, 147(3):379–413, 2010. MR-2639710

[BdT11] C. Boutillier and B. de Tilière. The critical Z-invariant Ising model via dimers: locality property. *Comm. in Math. Phys.*, 301(2):473–516, 2011. MR-2764995

[CDC13] David Cimasoni and Hugo Duminil-Copin. The critical temperature for the Ising model on planar doubly periodic graphs. *Electron. J. Probab.*, 18:no. 44, 18, 2013. MR-3040554

[CHI12] D. Chelkak, C. Hongler, and K. Izyurov. Conformal invariance of spin correlations in the planar Ising model. *ArXiv e-prints*, February 2012.

[CR07] D. Cimasoni and N. Reshetikhin. Dimers on surface graphs and spin structures. I. *Comm. Math. Phys.*, 275(1):187–208, 2007. MR-2335773

[CR08] D. Cimasoni and N. Reshetikhin. Dimers on surface graphs and spin structures. II. *Comm. Math. Phys.*, 281(2):445–468, 2008. MR-2410902

[dT07a] B. de Tilière. Quadri-tilings of the plane. *Probab. Theory Related Fields*, 137(3-4):487–518, 2007. MR-2278466

[dT07b] B. de Tilière. Scaling limit of isoradial dimer models and the case of triangular quadri-tilings. *Ann. Inst. H. Poincaré Probab. Statist.*, 43(6):729–750, 2007.

[Dub11a] J. Dubédat. Dimers and analytic torsion I. *ArXiv e-prints*, October 2011.

[Dub11b] J. Dubédat. Exact bosonization of the Ising model. *ArXiv e-prints*, December 2011.

[Duf68] R. J. Duffin. Potential theory on a rhombic lattice. *J. Combinatorial Theory*, 5:258–272, 1968. MR-0232005

[DZM$^+$96] N. P. Dolbilin, Yu. M. Zinov′ev, A. S. Mishchenko, M. A. Shtan′ko, and M. I. Shtogrin. Homological properties of two-dimensional coverings of lattices on surfaces. *Funktsional. Anal. i Prilozhen.*, 30(3):19–33, 95, 1996. MR-1435135

[Fan72] C. Fan. On critical properties of the Ashkin-Teller model. *Phys. Lett. A*, 39(2):136, 1972.

[Fis66] M. E. Fisher. On the dimer solution of planar Ising models. *J. Math. Phys.*, 7:1776–1781, October 1966.

[Ful95] W. Fulton. *Algebraic topology*, volume 153 of *Graduate Texts in Mathematics*. Springer-Verlag, New York, 1995. A first course. MR-1343250

[FW70] C. Fan and F. Y. Wu. General lattice model of phase transitions. *Phys. Rev. B*, 2:723–733, Aug 1970.

[GL99] A. Galluccio and M. Loebl. On the theory of Pfaffian orientations. I. Perfect matchings and permanents. *Electron. J. Combin.*, 6:Research Paper 6, 18 pp. (electronic), 1999. MR-1670286

[GV77] I. M. Gel′fand and N. Ya. Vilenkin. *Generalized functions. Vol. 4.* Academic Press [Harcourt Brace Jovanovich Publishers], New York, 1964 [1977]. Applications of harmonic analysis, Translated from the Russian by Amiel Feinstein.

[IR11] Y. Ikhlef and M. A. Rajabpour. Discrete holomorphic parafermions in the Ashkin–Teller model and SLE. *Journal of Physics A: Mathematical and Theoretical*, 44(4):042001, 2011. MR-2754707

[Kas61] P. W. Kasteleyn. The statistics of dimers on a lattice: I. the number of dimer arrangements on a quadratic lattice. *Physica*, 27:1209–1225, December 1961.

[Kas67] P. W. Kasteleyn. Graph theory and crystal physics. In *Graph Theory and Theoretical Physics*, pages 43–110. Academic Press, London, 1967. MR-0253689

[KB79] L. Kadanoff and A. C. Brown. Correlation functions on the critical lines of the Baxter and Ashkin-Teller models. *Ann. Phys.*, 121(1âĂŞ2):318–342, 1979.

[KC71] L. P. Kadanoff and H. Ceva. Determination of an operator algebra for the two-dimensional Ising model. *Phys. Rev. B*, 3:3918–3939, Jun 1971. MR-0389111

[Ken97] R. Kenyon. Local statistics of lattice dimers. *Ann. Inst. H. Poincaré Probab. Statist.*, 33(5):591–618, 1997. MR-1473567

[Ken02] R. Kenyon. The Laplacian and Dirac operators on critical planar graphs. *Invent. Math.*, 150(2):409–439, 2002. MR-1933589

[Ken04] Richard Kenyon. An introduction to the dimer model. In *School and Conference on Probability Theory*, pages 267–304. ICTP Lect. Notes, XVII, Abdus Salam Int. Cent. Theoret. Phys., Trieste, 2004. MR-2198850

[KOS06] R. Kenyon, A. Okounkov, and S. Sheffield. Dimers and amoebae. *Ann. of Math. (2)*, 163(3):1019–1056, 2006. MR-2215138

[KS05] R. Kenyon and J-M. Schlenker. Rhombic embeddings of planar quad-graphs. *Trans. Amer. Math. Soc.*, 357(9):3443–3458 (electronic), 2005. MR-2146632

[KW41a] H. A. Kramers and G. H. Wannier. Statistics of the two-dimensional ferromagnet. part I. *Phys. Rev.*, 60(3):252–262, Aug 1941. MR-0004803

[KW41b] H. A. Kramers and G. H. Wannier. Statistics of the two-dimensional ferromagnet. part II. *Phys. Rev.*, 60(3):263–276, Aug 1941. MR-0004804

[KW52] M. Kac and J. C. Ward. A combinatorial solution of the two-dimensional Ising model. *Phys. Rev.*, 88:1332–1337, Dec 1952.

[KW71] L. P. Kadanoff and F. J. Wegner. Some critical properties of the eight-vertex model. *Phys. Rev. B*, 4:3989–3993, Dec 1971.

[LG94] Zhi-Bing Li and Shou-Hong Guo. Duality for the Ising model on a random lattice and topologic excitons. *Nucl. Phys. B*, 413(3):723–734, 1994. MR-1262557

[Li10] Z. Li. Spectral Curve of Periodic Fisher Graphs. *ArXiv e-prints*, August 2010.

[Li12] Z. Li. Critical temperature of periodic Ising models. *Comm. Math. Phys.*, 315:337–381, 2012. MR-2971729

[Lie67] E. H. Lieb. Residual entropy of square ice. *Phys. Rev.*, 162:162–172, Oct 1967.

[Mas91] W.S. Massey. *A basic course in algebraic topology*, volume 127. Springer Verlag, 1991. MR-1095046

[Mau96] C.R.F. Maunder. *Algebraic topology*. Dover publications, 1996. MR-1402473

[Mer01] C. Mercat. Discrete Riemann surfaces and the Ising model. *Comm. Math. Phys.*, 218(1):177–216, 2001. MR-1824204

[MS] J. Miller and S. Sheffield. CLE(4) and the Gaussian Free Field. *(in preparation)*.

[Nie84] B. Nienhuis. Critical behavior of two-dimensional spin models and charge asymmetry in the Coulomb gas. *J. Statist. Phys.*, 34(5-6):731–761, 1984. MR-0751711

[Per69] J. K. Percus. One more technique for the dimer problem. *J. Math. Phys.*, 10(10):1881–1884, 1969. MR-0250899

[PS11] M. Picco and R. Santachiara. Critical interfaces and duality in the Ashkin-Teller model. *Phys. Rev. E*, 83:061124, Jun 2011.

[Sal87] H. Saleur. Partition functions of the two-dimensional Ashkin-Teller model on the critical line. *Journal of Physics A: Mathematical and General*, 20(16):L1127, 1987. MR-0924717

[SS09] O. Schramm and S. Sheffield. Contour lines of the two-dimensional discrete Gaussian free field. *Acta Math.*, 202(1):21–137, 2009. MR-2486487

[Sut70] B. Sutherland. Two-dimensional hydrogen bonded crystals without the ice rule. *J. Math. Phys.*, 11(11):3183–3186, 1970.

[Tes00] G. Tesler. Matchings in graphs on non-orientable surfaces. *J. Combin. Theory Ser. B*, 78(2):198–231, 2000. MR-1750896

[TF61] H. N. V. Temperley and M. E. Fisher. Dimer problem in statistical mechanics — an exact result. *Philosophical Magazine*, 6(68):1061–1063, 1961. MR-0136398

[Wan45] G. H. Wannier. The statistical problem in cooperative phenomena. *Rev. Mod. Phys.*, 17(1):50–60, Jan 1945.

[Weg72] F. J. Wegner. Duality relation between the Ashkin-Teller and the eight-vertex model. *J. of Phys. C: Solid State Physics*, 5(11):L131, 1972.

[Wil11] D. B. Wilson. XOR-Ising loops and the Gaussian free field. *ArXiv e-prints,* February 2011.

[WL75] F. Y. Wu and K. Y. Lin. Staggered ice-rule vertex model — the Pfaffian solution. *Phys. Rev. B*, 12:419–428, Jul 1975.

[Wu71] F. W. Wu. Ising model with four-spin interactions. *Phys. Rev. B*, 4:2312–2314, Oct 1971.

Electronic Journal of Probability
Electronic Communications in Probability

Advantages of publishing in EJP-ECP

- Very high standards

- Free for authors, free for readers

- Quick publication (no backlog)

Economical model of EJP-ECP

- Low cost, based on free software (OJS[1])

- Non profit, sponsored by IMS[2], BS[3], PKP[4]

- Purely electronic and secure (LOCKSS[5])

Help keep the journal free and vigorous

- Donate to the IMS open access fund[6] (click here to donate!)

- Submit your best articles to EJP-ECP

- Choose EJP-ECP over for-profit journals

---

[1] OJS: Open Journal Systems http://pkp.sfu.ca/ojs/
[2] IMS: Institute of Mathematical Statistics http://www.imstat.org/
[3] BS: Bernoulli Society http://www.bernoulli-society.org/
[4] PK: Public Knowledge Project http://pkp.sfu.ca/
[5] LOCKSS: Lots of Copies Keep Stuff Safe http://www.lockss.org/
[6] IMS Open Access Fund: http://www.imstat.org/publications/open.htm